Title
OPTIMIZATION OF STRENGTH AND TOUGHNESS IN A HIGH CARBON STEEL

Author
Kar, Rameshchandra J,

Publication Date
1976-12-01

LBL-5448
c.1

OPTIMIZATION OF STRENGTH AND TOUGHNESS IN A HIGH CARBON STEEL

Rameshchandra J. Kar
(M. S. thesis)

December 1976

Prepared for the U. S. Energy Research and Development Administration under Contract W-7405-ENG-48

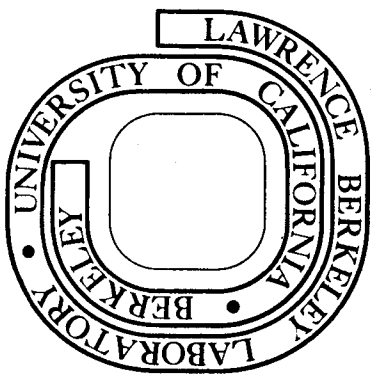

LBL-5448
c.1

DISCLAIMER

Table of Contents

OPTIMIZATION OF STRENGTH AND TOUGHNESS IN A HIGH CARBON STEEL

Rameshchandra J. Kar

Materials and Molecular Research Division, Lawrence Berkeley Laboratory
and Department of Materials Science and Engineering,
University of California, Berkeley, California 94720

ABSTRACT

In this investigation, ball-bearing grade E52100 steel and two of its Si modifications (1 wt% and 2 wt%Si) are examined for improved mechanical properties. Hardness, tensile and toughness testing have been done. Optical and scanning electron microscopy have been used to correlate microstructure with observed mechanical properties. It is found that use of high austenitization temperatures and/or Si modification give large amounts of retained austenite. Isothermal transformations subsequent to single or two-cycle austenitization give mixed microstructures of lower bainite, martensite and retained austenite. These offer the potential of achieving high strength-toughness combinations which could make this high carbon steel attractive for alternate applications.

I. INTRODUCTION

Commercial grade E 52100 has made its mark in the ball bearing industry. This high carbon steel (1% C) is characterized by a high hardness in the tempered martensitic condition. The age-old norm exists - the higher the carbon content, the higher the strength, but unfortunately, high carbon steels are extremely brittle.

Commercial usage of 52100 involves incomplete austenitization at relatively low temperatures, resulting in incomplete dissolution of alloy carbides, p-edominantly Fe-Cr complexes.[1] It is well known that undissolved carbides give poor toughness, particularly if these are incoherent and do not deform with the matrix.[2] The martensite formed on subsequent quenching is heavily twinned.[3] Twinned martensite is known to contribute to the strength of the alloy,[4] but it generally results in poor toughness.[5] Moreover, high carbon steels are plagued with the severe problem of microcracking. Microcracks appear at the tips of impinging martensitic plates and are a consequence of accommodation of transformation strains.[6] All these factors impart poor toughness.

In the spirit of a continuing program of alloy design for improved fracture toughness,[7] the present investigation is undertaken to develop optimum strength toughness combinations in this high carbon steel, by use of techniques that have met with a reasonable measure of success in steels of lower carbon content.

At the onset, it would be necessary to characterize the mechanical properties of 52100 in the quenched and tempered condition, following a typical austenitization schedule used in industry. This is because no systematic evaluation of this has been done, and the results obtained could serve as a basis of comparison for subsequent heat treatments.

Use of higher austenitization temperatures would dissolve alloy carbides but with greater carbon in solution, the microcracking tendency (which is a function of the carbon content) increases. Two cycle austenitization treatments have been suggested[8] to overcome this problem. It would be interesting to categorize the mechanical properties of quenched and tempered specimens using this technique.

However, the realm of isothermal transformations to lower bainite appears the most attractive treatment. Isothermal transformations offer the potential of achieving high strength-toughness combinations, since lower bainite has a morphology very similar to tempered martensite.[4] Thus investigations of lower bainite and duplux structures of lower bainite and martensite must be carried out, since these have exhibited good properties in other alloy steels.[9-12]

Addition of silicon and/or austenitization at high temperatures result in retention of large amounts of retained austenite.[13,14] It would be of interest to determine whether this austenite can be made to undergo a 'TRIP' phenomenon,[15] which could be used in conjunction with isothermal treatments to develop high strength-toughness combinations.

Thus this project aims at investigating different heat treatments in 52100 and its silicon variants, to impart reasonable toughness at

high strength and hardness levels that would make this high carbon steel attractive for alternate applications.

II. EXPERIMENTAL PROCEDURE

A. Material Preparation

The steels used in this investigation consist of three alloys - 52100 and two Si modifications viz. 52100 + 1 wt%Si and 52100 + 2 wt%Si. A part of the 52100 used was supplied by SKF Industries in the form of two 20 lb. ingots. The remainder of the 52100 and its Si variants were melted in a 100 kilowatt vacuum induction furnace and cast into 20 lb. ingots. The ingots were next flat forged at 1100°C to 0.56 in and 0.25 in plates. After sand blasting to remove oxide scale, the material was homogenized at 1200°C in vacuum for 48 hours and then furnace cooled. Chemical analysis were subsequently carried out on homogenized samples. The general compositions of the alloy are listed in Table 1.

B. Heat Treatment

Heat treatments were carried out on oversize round tensile, flat tensile, Charpy and three point bend test blanks, using a vertical tube furnace under argon atmosphere (Fig. 1). Quenching was carried out in agitated warm oil, or hot oil (150°C) as per the schedule used. Isothermal transformations were carried out in a large salt pot placed directly below the austenization furnace. The different heat treatments used are listed in Table II.

C. Mechanical Testing

1. Hardness Testing

Rockwell 'C' hardness tests were made on broken Charpy bars and bend test specimens, which were suitably prepared by metallographic polishing techniques prior to hardness testing. The hardness value reported corresponds to an average of six or more measurements.

Vickers microhardness values of some specimens were determined using a Leitz Wetzlar microhardness tester. An applied load of 1000 g. was used to make indentations on the specimen. Hardness was calculated from measurements of the indentation diagonals. Six or more measurements were made in each case.

2. Tensile Testing

Measurements of tensile properties were made using the 1 in. gage length, 0.25 in. diameter round specimen shown in Fig. 2. Oversize specimens were heat treated and then final ground to dimension under flood cooling. Tests were carried out at room temperature using a 300 Kip MTS at a loading rate of 0.04 in/min. A minimum of three tests were performed for each heat treatment. Most of the quenched and tempered specimens experienced failure in the linear elastic region and hence elongations have not been reported.

Tensile tests were also carried out on flat tensile specimens (Fig. 3) at room temperature using an Instron testing machine using a cross head speed of 0.05 cm/min.

3. Charpy Impact Testing

Oversize Charpy blanks were heat treated and then ground to final size and the V-notch inserted. Specimen dimensions and other details are given in Fig. 4. In all cases three specimens were tested for each heat treatment.

4. Fracture Toughness Testing.

Fracture toughness tests were carried out on heat treated bend test blanks which were ground to dimensions and a 0.008 in slot inserted (Fig. 5). Room temperature tests were carried out using a three-point bend test rig on the 300 Kip MTS, which is illustrated in Fig. 6.

The crack length was monitored using a crack opening displacement (COD) gage. Details of the calculations are given in the Appendix.

D. Dilatometry

Dilatometry was carried out on standard size dilatometric specimens using the Theta dilatometer (Fig. 7). The M_s, A_s and A_f temperatures of the alloy steels were established by dilatometry and are given in Table I.

The TTT diagrams of the three alloys were established by dilatometry by isothermal holding at different temperatures.

E. X-Ray Analysis

Measurements of retained austenite present at room temperature were carried out using the Picker X-ray diffractometer. Specimens were cut from broken Charpy and bend test bars. These were then polished and etched in a solution of 100 ml. H_2O_2 + 4 ml. HF to obtain a shiny

surface. The specimens were scanned using Cu K_α radiation and the $(111)_\gamma$ $(311)_\gamma$, $(220)_\gamma$, $(222)_\gamma$ reflections were measured.

Calculations of per cent retained austenite were made by the technique suggested by Miller,[16] with appropriate corrections being made for specimen composition.

F. Magnetic Tests

The saturation induction of specimens was measured before and during tensile testing. A schematic drawing of the permeameter is given in Fig. 8. Details of the calculations are given elsewhere.[17] Using this technique, it was possible to calculate the percentage of retained austenite present before testing, and the per cent that transformed to martensite during testing.

G. Optical Metallography

Optical metallography was carried out on specimens cut from Charpy and bend test pieces. These were mounted in Koldmount, suitably polished on silicon carbide papers down to 600 grit, polished on a 1 μ diamond abrasive wheel and then given a final polish with a 0.05 gamma micropolish in a Syntron. Specimens were etched using 2% nital or a solution of 5 gm. picric acid in a 100 cc solution of ethanol saturated with dodecylbenzene sulfonate.

H. Fractography

Examination of the fracture surfaces of Charpy bars and bend test specimens were done using an AMR scanning electron microscope at an

operating voltage of 20 kv. Fracture surfaces were protected with replicating tape during specimen preparation, which was subsequently dissolved in acetone.

III. RESULTS AND DISCUSSION

1. Preliminaries: Commercial heat treatments of 52100 involve austenitization at 840-900°C for 30-35 mins, followed by a warm oil quench and subsequent tempering. This results in undissolved carbides (Fig. 9a) which have been evaluated as complex Fe-Cr carbides.[1] It has been well established[18,19] that undissolved carbides are known to give poor fracture toughness and impact values, since these can act as crack nuclei. Hence it is evident that as a primary step towards improving toughness, higher austenitization temperatures than the schedule used in industry would be necessary. However high carbon steels are associated with the severe problem of microcracking,[20] which is a function of the size of the martensite packets formed on quenching.[21] In order to decrease this tendency towards microcracking, grain refinement techniques would be needed to be used in conjunction with high austenitization temperatures.

Silicon addition to low C steels such as 4340 has shown to increase resistance to softening during tempering[22] and to extend the temperature range in which ϵ carbide precipitates. It is also known to retard the 500°F embrittlement of tempered martensite.[23] It has also been known to cause retention of thermally-stabilized[24] retained austenite. Hence it was decided to investigate whether alloy modification of 52100 by Si addition in combination with different heat treatments could improve the mechanical properties. Table II explains the different heat treatments that have been used.

In particular, the primary objective was to improve the toughness of 52100 or its Si variants at strength and hardness levels utilized in the bearing industry.

2. Investigation of Quenched and Tempered Properties: Except for hardness measuremnts, practically no data is available on quenched and tempered treatments for 52100 steel. Hence as a starting point, austenitization treatments were carried out following a typical schedule used in industry (Schedule A). A schematic of the heat treatment is given in Fig. 10, and details in Table II. Various mechanical properties were measured and these are tabulated in Table IIIa. These are used as a basis for comparison of the different heat treatments which are discussed later.

As seen in Table IIIa, in the quenched and tempered condition, 52100 is extremely brittle, as indicated by the Charpy impact and fracture toughness test data. Tempering at 250°C for one hour gives a yield stress (corresponding to a 0.2% strain offset) of 227.8 ksi (1570.9 MPa), and ultimate tensile strength of 290 ksi (2000.5 MPa), at a hardness level of R_c 58 and a K_{Ic} value of 21.23 ksi-in$^{1/2}$ (23.3 MPa-m$^{1/2}$). The microstructure of as-quenched 52100 (Fig. 9a) shows presence of undissolved carbides, which clearly explains the low toughness at high strength levels, since these can act as crack nuclei.[18] X-ray measurements show that in the quenched and tempered condition (A-T250), 52100 has less than 5% retained austenite.

High carbon steels are generally associated with the problem of microcracking. This is considered to be a manifestation of the

formation of plate martensite.[25,26] Marder and Benscoter[26] identify the impingement of martensite plates within the bulk of a transforming specimen as a direct cause of microcracking. Figure 9b is a typical example of microcracks found in specimens heat treated as per schedule A. The moderate amount of microcracking is consistent with the results of others,[1] since dissolved carbon content exerts a strong influence on the microcracking sensitivity of high carbon alloys.[27]

In order to standardize treatments, and to study the effect of Si additions at low austenitization temperatures, one of the Si variants of 52100 viz. 52100 + 2 Si was subjected to the same schedule A, and properties measured in the quenched and tempered condition (Table IIIa). One of the interesting features is that addition of Si gives rise to a large amount of thermally-stabilized[24] retained austenite. Measurements of saturation induction during tensile testing show that the retained austenite undergoes a "stress-induced"[28] transformation to martensite before general yield has taken place. Addition of Si has severely retarded the tempering response (Fig. 11), so that at a tempering temperature of 250°C, 52100 + 2Si exhibits relatively lower Charpy impact and bend test values, at higher hardness levels when compared with unmodified 52100. Resistance to softening during tempering with addition of Si has also been observed in steels having a lower carbon content.[23]

Scanning fractography shows that as quenched 52100 + 2Si exhibits brittle transgranular fracture (Fig. 12). The fracture is primarily quasi-cleavage, having probably initiated at undissolved carbide particles.

Thus the above preliminary work done on quenched and tempered specimens shows that higher austenitization temperatures would be necessary to dissolve alloy carbide particles. However coupled with high austenitization temperatures the prior austenite grain size increases and a direct quench to room temperature gives rise to severe quench cracking. This is because severe microcracking occurs which results from the accommodation of strain at the tips of impinging plates.[21] The strain energy due to the volume change accompanying formation of martensite increases as the transformed volume and is proportional to the $(\text{length})^2 X$ thickness of the plate. In addition, the severity of the quench generates sufficient thermal stresses to aggravate quench cracking.

In order to dissolve the carbides, an optimum austenitization temperature of 1150°C was chosen. At this temperature all the complex Fe-Cr carbides are in solution. Austenitization at 1150°C was coupled with an interrupted quench in hot oil at 150°C (a temperature intermediate between M_s and M_f) and holding at this temperature for 5 mins. before cooling to room temperature. This was followed by a second austenitization treatment at 900°C in order to refine the prior austenite grain size. With a finer grain size, the greater is the energy absorbed during fracture and the more difficult is the process of crack propagation.[29] This also implies a larger grain boundary area and hence there is smaller coverage of grain boundaries by embrittling constituents.[30] Microcracking in quenched and tempered specimens would be controlled because of the finer plates formed on quenching.[29]

For the second cycle austenitization, an optimum time of 20 minutes was chosen, during which no carbon came out of solution, and the prior austenite grain size was fairly small. Figure 13 is a schematic of the two-cycle austenitization schedule for quenched and tempered treatments (termed Schedule B). Using this heat treatment the mechanical properties of quenched and tempered 52100, 52100+1Si, 52100+2Si have been measured and are given in Table IIIb.

Grange[29] has suggested that grain refinement by thermal cycling could improve the mechanical properties of 52100. However, as the results indicate, no significant improvement was obtained in the quenched and tempered condition. This is because of two opposing factors:

1. At low austenitization temperatures, undissolved carbides exist, which can act as crack nucleation sites.

2. At high austenitization temperatures, the microcracking tendency, which is a function of carbon content, increases. Although a two cycle austenitization treatment greatly reduces the amount of microcracking, the problem still persists because transformation strains at the tips of relatively smaller twinned martensitic plates still do exist.

As is seen in Fig. 14, there is a definite increase in the stress level at which specimens fracture (before general yield) in a tensile test. This is probably due to absence of undissolved alloy carbides and because microcracking has been reduced. In a comparison of fracture toughness (Fig. 15), two-cycle austenitized specimens show a slight improvement due to similar reasons.

Figures 16a, b, and c show the fracture surfaces of as-quenched 52100, 52100+1Si, and 52100+2Si, respectively. (Treatment B-AQ). As quenched 52100 shows intergranular fracture, with decohesion occurring along prior austenite grain boundaries; while 52100+1Si and 52100+2Si fail by quasi-cleavage. The occurrence of intergranular fracture in as-quenched 52100 is attributed to segregation of tramp elements such as P, Sb to grain boundaries during austenitization, since quasi-cleavage is the normal mode of fracture in 52100.[31] It has been suggested[30] that there is a temperature below which there is a sufficient thermodynamic driving force for segregation of the embrittling species to occur; and, that this temperature is essentially independent of grain size. The occurrence of a mixed mode (intergranular + quasi-cleavage) in quenched and tempered 52100 (Fig. 17a) in contrast to quasi-cleavage in the Si variants (Figs. 17b & c) is attributed to a similar reason.

Another interesting feature is that two-cycle austenitization leads to a large amount of retained austenite being entrapped at room temperature. Measurements of saturation induction during tensile testing indicate that the austenite undergoes a "stress-induced" transformation to martensite. However, since quenched and tempered test specimens break during tensile testing before general yield has taken place, no attempt is made to explain the effect of the "stress-induced" transformation of austenite to martensite on the yield point of the alloy being tested.

Thus a two-cycle austenitization treatment on quenched and tempered 52100 and its Si variants gives strength and hardness levels similar to those obtained at lower austenitization temperatures, with a slight improvement in toughness. It is possible that the retained austenite could be interposed between plates, and this is known to retard microcrack growth.[2] However the morphology cannot be established using optical microscopy and hence no definite conclusions can be made.

Classification of the quenched and tempered treatments has been done in order to serve as a source of comparison for isothermal treatments which are discussed next.

3. Investigation of Isothermal Treatments: If metastable austenite in a low alloy steel is held at a temperature above M_s, it decomposes isothermally into a product of deformed ferrite and carbide called bainite,[32] which closely resembles the structure of tempered martensite.[2] The bainite transformation exhibits feature common to both diffusion controlled and martensitic transformations.[33] It is this property that has made a large number of research workers follow the "bainitic route" to develop strength and toughness combinations in alloy steels.[10,11,12] In most alloy steels there are two distinct forms of bainite-upper and lower bainite. In upper bainite, which occurs at higher temperatures, carbide in the form of cementite precipitates between ferrite laths. Interlath carbides are known to cause embrittlement[34] and hence for strength-toughness combinations, decomposition of austenite to upper bainite is generally avoided. The structure of lower bainite consists of laths or plates of dislocated

ferrite with internal carbides and it is this morphology which offers scope for toughness at high strength levels.

A. Choice of Isothermal Temperatures

Thomas et al.[11,12] have suggested that lower bainitic structures may have properties superior to martensities, when the lower bainite is formed in high carbon steels by isothermal holding just above the M_s temperature. On the other hand, Holloman et al.[35] have reported bainitic structures to have inferior toughness when compared with tempered martensite, when isothermal holding is done above 370°C. These conflicting observations indicate that the temperature of isothermal holding is an important parameter, if optimum strength-toughness combinations are to be achieved.

Dilatometric investigations show that 52100 has a M_s temperature of 250°C (Table I), while addition of 1 wt% and 2 wt%Si tends to depress the M_s temperature to 244°C and 238°C, respectively. The M_s temperatures have been determined subsequent to austenitization at 900°C. The choice of 255°C as being one of the temperatures for isothermal holding appears natural since it is just a little higher than the M_s temperatures of the alloys. The second temperature selected was 50°C higher viz. 305°C. Stickels[1] has reported formation of films of proeutectoid carbide along grain boundaries, on isothermal holding at temperatures above 425°C. These would be deleterious to toughness, and hence an upper limit of 305°C was chosen, so that the austenite decomposition product would primarily be lower bainite. Details of the isothermal transformations carried out are given in Table II.

B. Isothermal Transformations Subsequent to Austenitization at 900°C

Figure 18 is a schematic diagram of Schedule C - isothermal holding for one hour after austenitization at 900°C for 1 hour. Isothermal treatments were carried out on 52100 and 52100+2Si at two different temperatures viz. 255°C and 305°C. Various properties evaluated are listed in Table IV. Figures 19, 20 and 21 are the TTT diagrams of the alloys which have been determined by dilatometry.

(i) 52100 - Isothermal at 255°C: On isothermal holding at 255°C for 1 hour after austenitization at 900°C (C-I255), 52100 exhibits a yield strength of 210.8 ksi (1453.7 MPa) and ultimate tensile strength of 312.4 ksi (2154.3 MPa), at a hardness level of R_c 50. It has a Charpy impact value of 7.7 ft-lbs (10.43 joules) and plane strain fracture toughness of 25.5 ksi-$in^{1/2}$ (28.05 MPa-$m^{1/2}$). X-ray measurements do not reveal appreciable amounts of retained austenite (less than 5%).

Figure 22a shows the microstructure, which is a duplex structure of lower bainite and twinned martensite, as determined from the TTT diagram (Fig. 19). This duplex structure which is primarily lower bainite, exhibits slightly higher toughness than the twinned martensite found in quenched and tempered 52100, when compared at similar strength levels. High toughness values in duplex structures have also been observed by others.[8]

Examination of the fracture surface (Fig. 22b) shows a mixed mode of fracture - partly intergranular and partly quasi-cleavage. Fracture probably initiates at undissolved carbide particles which can act as stress raisers and crack nucleators, especially if the carbides are

non-coherent and do not deform with the matrix.[2] Segregation of impurities to prior austenite grain boundaries could be the reason for the appearance of partial intergranular fracture.

(ii) 52100 - Isothermal at 305°C: On raising the temperature of isothermal holding to 305°C (Heat treatment C-I305), a slight decrease in yield and ultimate tensile strength, with an attendant increase in impact and fracture toughness is observed (Table IV). The usual strength toughness behavior is similar to that reported by Huang et al.[12] ie. with an increase in temperature of isothermal holding, the strength decreases with a corresponding increase in toughness. Referring to the TTT diagram (Fig. 19), it appears that the microstructure (Fig. 22c) is completely lower bainitic since X-ray measurements did not reveal appreciable amounts of retained austenite.

Figure 22d shows that fracture occurs primarily by quasi-cleavage. Some secondary cracks are also seen, which are due to local decohesion occurring when undissolved alloy carbides do not deform with the matrix.

(iii) 52100+2Si - Isothermal at 255°C: Addition of 2 wt%Si to 52100 causes a large increase in the amount of retained austenite present at room temperature. (Heat Treatment C-I255). As indicated in Table IV 52100+2Si exhibits similar levels of yield and ultimate tensile strength (within limits of experimental scatter). However, with addition of Si, there is a large increase in plane strain fracture toughness from 25.5 ksi-in$^{1/2}$ (28.05 MPa-m$^{1/2}$) to 35.88 ksi-in$^{1/2}$ (39.42 MPa-m$^{1/2}$). Measurements of saturation induction indicate that a part of the retained austenite is undergoing a "strain-induced" transformation to

martensite during tensile testing. Austenite is a ductile phase which can effectively blunt propagating cracks. It has been suggested[15] that austenite of the right stability can transform to martensite resulting in energy absorption ahead of a moving crack. This explains the increase in toughness observed.

From the TTT diagram (Fig. 21) it is seen that the microstructure (Fig. 23a) consists of a duplex structure of lower bainite and twinned martensite, with some amount of retained austenite. This explains the high hardness since twinning increases the strength of metals and in steels, it is additive to the strengthening from the carbon in solution.[2]

Scanning fractography (Fig. 23b) shows that 52100+2Si subjected to heat treatment C-I255 displays quasi-cleavage. Similar fracture surfaces have also been reported elsewhere.[31,36]

(iv) 52100+2Si - Isothermal at 305°C: Isothermal holding at 305°C for 1 hour (heat treatment C-I305), gives a lower bainitic structure in 52100+2Si (Fig. 23c), with an appreciable amount of retained austenite also being present. An increase in temperature of isothermal holding has caused a decrease in tensile properties (Table IV), while the impact toughness has registered a sharp increase (the K_{Ic} remains almost the same - a fact which indicates that higher impact resistance need not necessarily quarantee higher K_{Ic} values).

Examination of the fracture surface (Fig. 23d) shows a mixed mode of failure - quasi-cleavage + dimpled rupture. Low[37] has attributed this fracture morphology to a void-coalescence mechanism. The mixed mode of fracture indicates that when a cleavage crack is arrested,

some deformation and ductile fracture occurs until a new crack is initiated,[38] which explains the relatively high impact toughness value. Energy absorption by the ductile phase (austenite) ahead of the crack front as it transforms to martensite under applied strain, also remains a possibility.

Thus isothermal treatments at temperatures close to M_s after low temperature austenitization indicate that lower bainite, when present in a duplex structure offers the potential of higher toughness than quenched and tempered treatments, when compared at similar strength levels. Similar results have also been reported by others.[12,39]

C. Isothermal Treatments Subsequent to Two Cycle Austenitization

Low temperature austenitization of 52100 has the inherent disadvantage of undissolved alloy carbides being present in the microstructure. Two-cycle austenitization treatments offer the possibility of dissolving the carbides, which are known to be deleterious to toughness. At the same time, since carbon in solution is an important parameter governing the strength of the steel,[39] higher strength levels are feasible. A small grain size at the end of the second cycle austensitization allows greater energy absorption during fracture and a more difficult process of crack propagation.[40] When coupled with isothermal transformations at temperatures close to M_s, high strength-toughness combinations could be envisaged, since similar treatments at lower austenitization temperatures have shown encouraging results. The details of the heat treatment are given in Table 1, while Fig. 24 is a schematic of the schedule (termed D).

The mechanical properties using different isothermal temperatures on the alloy systems are given in Table V.

(i) 52100 - Isothermal at 255°C: Two-cycle austenitization coupled with isothermal holding at 255°C for 1 hour (heat treatment D-I255) causes a sharp increase in the yield and ultimate tensile strengths of 52100 from 210.8 ksi (1453.7 MPa) and 312.4 ksi (2154.3 MPa) (in treatment C-I255) to 246 ksi (1696.4 MPa) and 331 ksi (2282.6 MPa) respectively. At the same time the plane strain fracture toughness has increased from 25.5 ksi-$in^{1/2}$ (28.05 MPa-$m^{1/2}$) to 46.22 ksi-$in^{1/2}$ (50.78 MPa-$m^{1/2}$).

Figure 25a shows the microstructure which consists essentially of lower bainite coupled with twinned martensite and retained austenite. (This was verified by subsequent microhardness measurements of the different microconstituents.)

The increase in yield strength can be explained as being due to the greater amount of carbon in solution. The effect of a fine prior austenite grain size is well known.[41] The concomitant increase in fracture toughness is attributed to the following factors:

1. Absence of undissolved alloy carbides, which can cause cracking, particularly if they are non-coherent and cannot deform with the matrix.

2. The large amount of retained austenite present at room temperature. Saturation induction measurements indicate that a part of the retained austenite transforms to martensite under strain (Table VI). This effect partly accounts for the higher impact and fracture toughness values observed.

3. The fine prior austenite grain size restricts the size of the laths or plates of dislocated ferrite in bainite and the twinned martensitic plates, thus making crack propagation more difficult.[40]

Examination of the fracture surface (Fig. 25b), shows characteristic quasi-cleavage, with no traces of intergranular fracture detected in treatment C-I255.

(ii) 52100 - Isothermal at 305°C: Two-cycle austenitization, followed by isothermal holding at 305°C for 1 hour (heat treatment D-I305), causes a slight drop in yield and ultimate tensile strengths, with an increase in fracture toughness to 62.1 ksi-in$^{1/2}$ (68.23 MPa-m$^{1/2}$) in comparison with the previous heat treatment. This type of strength toughness behavior with increasing isothermal transformation temperature has also been reported by others.[12]

The microstructure is shown in Fig. 25c while Fig. 25d is a scanning fractograph. Fracture has occurred primarily by quasi-cleavage.

Measurements of saturation induction during tensile testing (Table VI) indicate that a part of the retained austenite is undergoing a strain induced transformation to martensite.

(iii) 52100+1Si - Isothermal at 255°C: Addition of 1% Si has altered the kinetics of the bainite transformation so that isothermal holding at 255°C for 1 hour (D-I255) gives a microstructure of lower bainite with some amount of retained austenite. This explains the decrease in strength and hardness, since twinned martensite which contributes to the strength of the alloy[2] is absent. A high toughness value is observed characteristic of a lower bainitic structure.

Figures 26a and 26b are photographs of the microstructure and fracture surface respectively.

(iv) 52100+1Si - Isothermal at 305°C: An increase in temperature of isothermal holding to 305°C (D-I305) causes a slight increase in the amount of retained austenite present at room temperature. Saturation induction measurements indicate that a part of the austenite undergoes a "strain-induced" transformation to martensite which partly accounts for the high K_{Ic} value observed - 67.5 ksi-in$^{1/2}$ (74.16 MPa-m$^{1/2}$).

The microstructure is illustrated in Fig. 26c. Examination of the fracture surface (Fig. 26d) shows that the fracture mode is quasi-cleavage.

(v) 52100+2Si - Isothermal at 255°C: One of the interesting features is that the addition of a further amount of Si seems to have altered the kinetics of the bainite reaction, so that isothermal holding of 52100+2Si at 255°C for 1 hour (D-I255) produces a mixed microstructure of lower bainite and martensite, with an appreciable amount of retained austenite, as ascertained by X-ray measurements. This is illustrated in Fig. 27a. The superior mechanical properties exhibited by this treatment corroborate the findings of Hehemann[33] and others[11,12] that isothermal holding just above the M_s temperature produces a combination of strength and toughness superior to quenched and tempered treatments.

The fracture surface is illustrated in Fig. 27b. Quasi-cleavage is the mode of fast fracture.

(vi) 52100+2Si - Isothermal at 305°C: Two-cycle austenitization coupled with isothermal holding at 305°C for 1 hour results in an

increase in fracture toughness in 52100+2Si, when compared to D-1255 with the yield and ultimate tensile strength remaining at the same levels. The microstructure consists of a duplex structure of lower bainite and martensite (probably twinned), and some retained austenite. This is illustrated in Fig. 27c. With about 25% of the matrix being austenitic, it is understandable that the fracture toughness should be fairly high, since austenite is a ductile phase and it can effectively blunt any cracks that occur in the microstructure.

Examination of the fracture surface (Fig. 27d) shows quasi-cleavage, typical of high carbon steels.

D. Summary of Results for Isothermal Treatments

Figure 28 is a comparative plot of hardness measurements for the various isothermal treatments that have been carried out on 52100, 52100+1Si, and 52100+2Si. Presence of a mixed microstructure gives higher hardness levels, with a slight reduction in hardness as the temperature of isothermal holding is raised. Heat treatments D-I255 and D-I305 in 52100+1Si exhibit lower hardness when compared with the same treatments in the other two alloys. This is because addition of 1 wt%Si has altered transformation kinetics, so that isothermal holding for 1 hour does not produce a duplex structure in this alloy. The exact reason for this phenomenon cannot be established due to lack of available information.

Mixed microstructures produced by two-cycle austenitization isothermal holding exhibit higher yield and ultimate tensile strengths than do lower bainitic structures as is illustrated in Fig. 29. It

would not be out of bounds to speculate that this is due to the martensite, (one of the microconstituents of the mixed structures) being heavily twinned.

With higher temperatures of isothermal holding, there is an increase in fracture toughness, as is illustrated in Fig. 30. This is consistent with the reports of others.[11,12]

Figure 31 illustrates the variation in retained austenite at different stages of tensile testing. It appears that a part of the retained austenite is undergoing a "strain-induced" transformation to martensite as the measurements of saturation induction indicate.

The various fracture toughness-strength combinations that have been obtained are plotted in Fig. 32. When compared with the fracture toughness-strength combination that is possible in quenched and tempered 52100, it is evident that superior combinations have been obtained through the use of isothermal treatments.

IV. CONCLUSIONS

Based on experimental observations and results, the following conclusions are made:

1. In the quenched and tempered condition, after low temperature austenitization, 52100 is extremely brittle, because of the presence of undissolved alloy carbides and microcracks in a twinned martensitic microstructure.

2. Austenitization temperatures greater than 1100°C are necessary to dissolve alloy carbides. However a direct quench to room temperature produces severe cracking.

3. A two-cycle austenitization treatment which consists of austenitization at a high temperature, an interrupted quench and reaustenitization to a lower temperature to refine the prior austenite grain size, does not give any significant improvement in the mechanical properties of 52100 or its Si modifications, in the quenched and tempered condition.

4. Additions of Si and/or two-cycle austenitization treatments, severely retard the tempering response at low tempering temperatures.

5. Additions of Si and/or two-cycle austenitization treatments cause large amounts of retained austenite to be present at room temperature.

6. Isothermal transformations at temperatures close to M_s after low temperature austenitization, produce better fracture toughness, in comparison with quenched and tempered treatments (at similar strength levels).

7. Additions of differing amounts of Si alter the kinetics of the bainite transformation to different extents.

8. Isothermal transformation subsequent to two-cycle austenitization are found to give strength-toughness combinations superior to quenched and tempered treatments.

9. The mixed microstructures of lower bainite and martensite produced by isothermal transformations subsequent to two-cycle austenitization exhibit high strength because a greater amount of carbon is in solution and because twinned martensite is probably one of the microconstitutents.

10. Measurements of saturation induction confirm that a part of the retained austenite undergoes a "strain-induced" transformation to martensite. This, coupled with absence of undissolved carbides and blunting effect of the ductile phase (austenite) could explain the improved toughness.

11. On raising the temperature of isothermal holding, the usual strength toughness behavior is observed viz. the fracture toughness increases with an attendant decrease in yield and ultimate tensile strengths.

ACKNOWLEDGEMENTS

The author would like to thank Professors E. R. Parker and V. F. Zackay for their continuing encouragement and support throughout the course of this project, and Professor F. Hauser for his review of the manuscript.

The unending help and suggestions offered by a large number of people from the 'P-Z' group deserves special mention. In particular the author would like to thank Dr. R. O. Ritchie, R. M. Horn, M. S. Bhat, Tom Lechtenberg and Naresh Kar for their valuable suggestions and ideas.

Special thanks are due to the support staff and technical personnel of the Materials and Molecular Research Division, with special mention of E. Edwards and J. A. Patenaude (machine shop), Don Krieger (mechanical testing), S. Stewart (purchasing), E. Grant (technical illustrations) and Alice Ramirez (technical typing).

Finally, the author would like to thank his parents and the rest of his family without whose encouragement this project would not have been possible.

This project was performed under the auspices of the U.S. Energy Research and Development Administration through the Materials and Molecular Research Division of the Lawrence Berkeley Laboratory.

APPENDIX

Fracture Toughness Testing

The bend test specimens that were used for fracture toughness testing by three point bending were designed according to ASTM specifications.[42] However it was not possible to fatigue pre-crack the specimens ($\rho \to 0$) and hence the specimens were tested with a machined crack having a root radius of 0.004 in. Although these tests, were not valid, as per ASTM specifications, these serve as an effective means of comparing the toughnesses for different heat treatments, since for high strength, low ductility alloys, Charpy Impact tests (static) are not sensitive enough to respond to small changes in toughness.

The apparent fracture toughness K_{app} was calculated as:

$$K_{app} = [P_Q S/BW^{3/2}]\ f(a/w)$$

where

$$f(a/W) = [2.9(a/W)^{1/2} - 4.6(a/W)^{3/2} + 21.8(a/W)^{5/2} - 37.6(a/W)^{7/2} + 38.7(a/W)^{9/2}]$$

where P_q = load

B = thickness of specimen

S = span length

W = depth of specimen

a = crack length

As has been suggested by Heald et al.,[43] the plane strain fracture toughness K_{Ic} was calculated from the apparent fracture toughness as:

$$K_{Ic} = \left[8\,\sigma_u^2 \times 0.19\ \ell n \sec \left(\frac{1.145\ K_{app}^{\pi/2}}{\sigma_u (\pi \times 0.19)^{1/2}} - \frac{\pi \times 0.145}{2} \right) \right]^{1/2}$$

where K_{app} = apparent fracture toughness

σ_u = ultimate tensile strength

REFERENCES

1. C. A. Stickels, Met. Trans. 5, 865 (1974).
2. G. Thomas, Iron and Steel International 46, 451 (1973).
3. R. A. Grange, Met. Trans. 2, 65-78 (1971).
4. G. Thomas, Met. Trans. 2, 2379 (1971).
5. E. R. Parker and V. F. Zackay, Eng. Fract. Mech. 7, 371 (1975).
6. R. P. Brobst and G. Krauss, Met. Trans. 5, 457 (1974).
7. V. F. Zackay and E. R. Parker, LBL-2782, Lawrence Berkeley Laboratory, University of California, Berkeley, California (1974).
8. B. V. N. Rao, M.S. Thesis, LBL-3794, University of California, Berkeley, California (1975).
9. K. J. Irvine and F. B. Pickering, J. Iron & Steel Inst. (London) 201, 518 (1963).
10. R. F. Hehemann, V. J. Luhan and A. R. Troiano, Trans. ASM 49, 409-427 (1957).
11. S. K. Das and G. Thomas, Trans. ASM 62, 659 (1969).
12. D. H. Huang and G. Thomas, Met. Trans. 2, 1587-1598 (1971).
13. B. N. P. Babu, D. Eng. Thesis, LBL-2772, University of California, Berkeley, California (1974).
14. G. Y. Lai, W. E. Wood, R. A. Clark, V. F. Zackay and E. R. Parker, Met. Trans. 5, 1663 (1974).
15. V. F. Zackay, M. D. Bhandarkar and E. R. Parker, LBL-2775, University of California, Berkeley, California (1974).
16. R. L. Miller, Trans. ASM 57, 892-899 (1964).

17. Bertrand de Miramon, M.S. Thesis, University of California, Berkeley, California, September (1967).

18. V. F. Zackay, E. R. Parker, J. W. Morris and G. Thomas, Mat. Sci. and Engn. 16, 201 (1974).

19. V. F. Zackay, E. R. Parker, R. D. Goolsby and W. E. Wood, Nature Phys. Sciences, 236, 108 (1972).

20. A. R. Marder and A. O. Benscoter, Trans. ASM 61, 293 (1968).

21. R. G. Davies and C. L. Magee, Met. Trans. 3, 307 (1972).

22. C. J. Alstetter, M. Cohen and B. L. Averbach, Trans. ASM 55, 287-300 (1962).

23. G. R. Speich and W. C. Leslie, Met. Trans. 3, 1043-1054 (1972).

24. E. P. Klier and A. R. Troiano, Metals Technology, 12, 1 (1945).

25. R. G. Davies and C. L. Magee, Met. Trans. 3, 312 (1972).

26. A. R. Marder and A. O. Benscoter, Met. Trans. 1, 3234 (1970).

27. M. G. Mendiratta, J. Sasser and G. Krauss, Met. Trans. 3, 351 (1972).

28. B. L. Averbach, S. Lorris and M. Cohen, Trans. ASM 44, 746 (1952).

29. R. A. Grange, Trans. ASM 62, 1024-1027 (1969).

30. G. Clark, R. O. Ritchie and J. F. Knott, Nature Physical Science, 239-94, 104-106 (1972).

31. Metals Handbook Vol. 9, Fractography and Atlas of Fractographs - 8th Edition, American Society for Metals, Metals Park, Ohio (1974).

32. G. Thomas, loc. sit vide ref. 2 (1973).

33. R. F. Hehemann, ASM Seminar "Phase Transformations," Metals Park, Ohio, p. 397 (1970).

34. G. Y. Lai, Met. Trans. 6A, 1469-1471 (1975).

35. J. H. Holloman, L. D. Jaffe, D. E. McCarthy and M. R. Norton, ASM Trans. (Quarterly), 58, 807 (1947).

36. K. Sipos, L. Remy and A. Pineau, Met. Trans. 7A, 857-864 (1976).

37. J. R. Low, Jr., Eng. Fracture Mech. 1, 47 (1968).

38. F. B. Pickering, Symposium: Transformation and Hardenability in Steels, p. 109, Climax Molybdenum Co., (1967).

39. R. Brock and J. E. Russell, Special Report 86, p. 20, Iron and Steel Institute, England (1964).

40. J. R. Low, Jr., Fracture, p. 68, MIT Press, Cambridge, Mass. (1959).

41. N. J. Petch, Phil. Mag. 3, 1089 (1958).

42. Annual of ASTM Standards, E 399, American Society for Testing of Materials, PA. (1973).

43. P. Heald, G. Spink and P. Worthington, Mat. Sci. & Eng. 10, 129 (1972).

Table I. Alloy Compositions.

C Wt%	Si Wt%	Cr Wt%	Mn Wt%	Fe Wt%	M_s °C	A_s °C	A_f °C
1.0	0.19	1.35	0.32	Bal.	250	740	772

E-52100 + 1Si

C Wt%	Si Wt%	Cr Wt%	Mn Wt%	Fe Wt%	M_s °C	A_s °C	A_f °C
1.0	1.19	1.35	0.32	Bal.	244	762	791

E-52100 + 2Si

C Wt%	Si Wt%	Cr Wt%	Mn Wt%	Fe Wt%	M_s °C	A_s °C	A_f °C
1.0	2.19	1.35	0.32	Bal.	235	790	823

Table II. Heat Treatment Details.

	Symbol	Treatment
1.	A-AQ	Austenitization at 900°C 1hr → warm oil quench (55°C)
2.	A-T150	1 + Temper 150°C 1hr.
3.	A-T200	1 + Temper 200°C 1hr.
4.	A-T250	1 + Temper 250°C 1hr.
5.	B-AQ	Austenitization at 1150°C 1hr → Interrupted Quench (Hot Oil 150°C) 5 mins → R.T. → Austenitization at 900°C 20 mins → Oil Quench.
6.	B-T150	5. + Temper 150°C 1hr
7.	B-T200	5. + Temper 200°C 1hr
8.	B-T250	5. + Temper 250°C 1hr
9.	C-I255 (or C-Isoth 255°C)	Austenitization at 900°C 1hr → Isothermal holding at 255°C 1hr → Quench to R.T.
10.	C-I305 (or C-Isoth 305!C)	Austenitization at 900°C 1hr → Isothermal holding at 305°C 1hr → Quench to R.T.
11.	D-I255 (or D-Isoth 255°C)	Austenitization at 1150°C 1hr → Interrupted Quench (Hot Oil 150°C) 5mins → R.T. → Austenitization at 900°C 20 mins → Isothermal holding at 255°C 1hr → Quench to R.T.
12.	D-I305 (or D-Isoth 305°C)	Austenitization at 1150°C 1hr → Interrupted Quench (Hot Oil 150°C) 5 mins → R.T. → Austenitization at 900°C 20 mins → Isothermal holding at 305°C 1hr → Quench to R.T.

Table III(a). Schedule A-Quenched and Tempered

Alloy	Treatment	TENSILE PROPERTIES						FRACTURE PROPERTIES					
		0.2 Pct Proof Stress		Ultimate Tensile Strength		Fracture Stress		Charpy V-Notch Impact Energy		Apparent Fracture Toughness		%Retained Austenite	Hardness R_c
		(ksi)	(MPa)	(ksi)	(MPa)	(ksi)	(MPa)	(ft-lbs)	(Joules)	(ksi-$in^{1/2}$)	(MPac-$m^{1/2}$)		
52100:	1. A-AQ	Broke before general yield				160.1	1104.0	5.0	6.78	19.47	21.39	5.0	64.4
	2. A-T150	- do		-		174.8	1205.4	5.4	7.32	28.38	31.18	5.0	63.1
	3. A-T200	- do		-		229.9	1585.3	6.0	8.14	37.29	40.97	5.0	59.8
	4. A-T250	227.8	1570.9	290.1	2000.5	290.1	2000.5	6.2	8.41	42.57*	46.77*	-	58
52100+ 2Si:	1. A-AQ	Quench Cracked				-	-	1.25	1.70	17.94	19.71	17.5	64.5
	2. A-T150	Broke before general yield				118.2	815.1	1.88	2.55	23.10	25.38	13.7	62.3
	3. A-T200	- do		-		143.5	989.6	2.75	3.73	31.80	34.94	10.7	60.5
	4. A-T250	- do		-		190.8	1315.7	4.25	5.76	36.44	40.03	5.3	59.5

*Has a corresponding plane strain fracture toughness K_{Ic} = 21.23 ksi-$in^{1/2}$ (23.3 MPa-$in^{1/2}$)

Table III(b). Schedule B-Quenched and Tempered

ALLOY	TREATMENT	TENSILE PROPERTIES		FRACTURE PROPERTIES				%RETAINED AUSTENITE	HARDNESS R_c
		Fracture Stress		Charpy V-Notch Impact Energy		Apparent Fracture Toughness			
		(ksi)	(MPa)	(Ft-lbs)	(Joules)	(ksi-$in^{1/2}$)	(MPa-$in^{1/2}$)		
52100	1. B-AQ	202.1	1393.7	5.0	6.78	21.70	23.84	36	63.5
	2. B-T150	220.0	1517.1	5.5	7.45	28.20	30.98	33.5	63
	3. B-T200	256.0	1765.4	5.6	7.59	38.60	42.41	26.2	61
	4. B-T250	275.3	1898.5	5.8	7.86	44.67	49.08	16.0	60
52100+1Si	1. B-AQ	150.0	1034.4	5.0	6.78	14.08	15.47	41.0	63
	2. B-T150	167.7	1156.4	5.6	7.59	22.33	24.53	40.2	62
	3. B-T200	192.5	1327.5	5.7	7.73	28.08	30.85	40.1	60.5
	4. B-T250	227.9	1571.6	5.9	7.99	41.09	45.14	40.0	60
52100+2Si	1. B-AQ	105.2	725.5	5.0	6.78	17.15	18.84	43.2	63
	2. B-T150	138.3	953.7	5.6	7.59	22.25	24.44	43.0	61
	3. B-T200	178.7	1232.3	5.8	7.86	24.36	26.76	42.2	60
	4. B-T250	223.6	1541.9	5.9	7.99	38.29	42.07	40.5	59.9

Table IV. Schedule C-Isothermal Treatments

Alloy	Treatment	Tensile Properties				Fracture Properties						%Retained Austenite (Unstressed)	Hardness R_c
		0.2 Pct Proof Stress (ksi)	(MPa)	Ultimate Tensile Strength (ksi)	(MPa)	Fracture Stress (ksi)	(MPa)	Charpy V-notch Impact Toughness (ft-lbs)	(Joules)	Plane Strain Fracture Toughness K_{Ic} (ksi-in$^{1/2}$)	(MPa-in$^{1/2}$)		
52100	1. C-I255	210.8	1453.7	312.4	2154.3	312.4	2154.3	7.7	10.43	25.53	28.05	5.0	50
	2. C-I305	229.0	1579.2	279.2	1925.4	220	1517.1	9.5	12.88	71.82	78.91	5.0	48
52100 +2Si	1. C-I255	210.0	1448.1	290.0	1999.8	290.0	1999.8	5.5	7.46	35.88	39.42	18.30	56
	2. C-I305	185.0	1275.8	230.0	1586.1	230.0	1586.1	11.0	14.91	34.27	37.65	16.0	46

Table V. Schedule D-Isothermal Treatments

Alloy	Treatment	Tensile Properties						Charpy V-notch Impact Toughness		Plane Strain Fracture Toughness K_{Ic}		%Retained Austenite (Unstressed)	Hardness R_c
		0.2 Pct Proof Stress (ksi)	(MPa)	Ultimate Tensile Strength (ksi	(MPa)	Fracture Stress (ksi)	(MPa)	(ft-lbs)	(Joules)	(ksi-$in^{1/2}$)	(MPa-$in^{1/2}$)		
52100	1. D-I255	246.0	1696.4	331.0	2282.6	331.0	2282.6	8.7	11.83	46.22	50.78	22.3	56
	2. D-I305	205.0	1413.7	257.0	1772.3	223.0	1537.8	8.9	12.01	62.1	68.23	24.9	52
52100 +1Si	1. D-I255	182.5	1258.5	232.1	1600.6	232.1	1600.6	6.6	8.95	46.8	51.42	22.0	47
	2. D-I305	177.4	1223.3	237.7	1639.2	237.7	1639.2	8.8	11.92	67.5	74.16	25.2	45
52100 +2Si	1. D-I255	203.5	1403.4	254.4	1754.3	254.4	1754.3	6.0	8.13	35.1	38.56	22.3	54
	2. D-I305	205.4	1416.5	259.1	1786.7	259.1	1786.7	8.2	11.11	61.2	67.24	26.6	49

Table VI. %Retained Austenite Measurements for Isothermal Treatments Stages of Tensile Testing.

Alloy	Treatment	Per Cent Retained Austenite		
		Unstressed	At Yield (0.2 Pct Proof Stress)	At 2% Strain
52100	1. D-I255	22.3	22.2	20.7
	2. D-I305	24.9	24.8	23.4
52100 +1Si	1. D-I255	22.0	21.9	20.4
	2. D-I305	25.2	25.1	23.6
52100 +2Si	1. C-I255	18.3	18.1	16.6
	2. C-I305	16.0	15.8	14.3
	3. D-I255	22.3	22.2	20.7
	4. D-I305	26.6	26.5	25.1

Table VII. Calculations of K_{Ic} values from K_{app} data.

Alloy	Treatment	Ultimate Tensile Strength (ksi)	Ultimate Tensile Strength (MPa)	Apparent Fracture Toughness K_{app} (ksi-in$^{1/2}$)	Apparent Fracture Toughness K_{app} (MPa-in$^{1/2}$)	Plane Strain Fracture Toughness K_{Ic}* (ksi-in$^{1/2}$)	Plane Strain Fracture Toughness K_{Ic}* (MPa-in$^{1/2}$)
52100	1. A-T250	290.1	2000.5	42.57	46.77	21.23	23.31
	2. C-I255	312.4	2154.3	53.25	58.50	25.53	28.05
	3. C-I305	279.2	1925.4	88.46	97.18	71.82	78.91
	4. D-I255	331.0	2282.6	72.47	79.61	46.22	50.78
	5. D-I305	257.0	1772.3	77.98	85.67	62.1	68.23
52100 +1Si	1. D-I255	232.1	1600.6	63.11	69.34	46.8	51.42
	2. D-I305	237.7	1639.2	80.1	88.0	67.5	74.16
52100 +2Si	1. C-I255	290.0	1999.8	59.55	65.42	35.88	39.42
	2. C-I305	230.0	1586.1	52.21	57.36	34.27	37.65
	3. D-I255	254.4	1754.3	55.5	60.97	35.1	38.56
	4. D-I305	259.1	1786.7	77.7	85.36	61.2	67.24

*calculations based on

$$K_{Ic} = \{8\sigma_u^2 \times 0.19 \ln \sec [\frac{1.145 K_{app} \cdot \pi/2}{\sigma_u \sqrt{\pi \times 0.19}} - \frac{\pi}{2} \times 0.145]\}^{1/2}$$

(ref. Heald, et al[43])

FIGURE CAPTIONS

Fig. 1. Heat treatment furnaces.

Fig. 2. Round tensile specimen.

Fig. 3. Flat tensile specimen.

Fig. 4. Charpy V-notch specimen.

Fig. 5. Three point bend-test specimen.

Fig. 6. MTS rig used for three-point bending. Inset shows set-up details.

Fig. 7. Theta dilatometer and associated controls.

Fig. 8. Schematic of the magnetic saturation apparatus.

Fig. 9. a) Microstructure of 52100 which has been austenitized at 900°C, oil quenched and tempered at 250°C. Microstructure shows a large amount of undissolved carbides.

b) Microcracks in quenched and tempered 52100 as seen at (a), (b), (c), (d), and (e).

Fig. 10. Schematic of Schedule A - quenched and tempered heat treatment used in industry.

Fig. 11. Hardness v/s tempering temperature for 52100, 52100+1Si, 52100+2Si, subsequent to single cycle austenitization (A) and two cycle austenitization (B).

Fig. 12. Scanning fractograph of as-quenched 52100+2Si which shows brittle transgranular fracture.

Fig. 13. Schematic of Schedule B - two cycle austenitization coupled with quenching and tempering.

Fig. 14. Fracture stress v/s tempering temperature for quenched and tempered heat treatments.

Fig. 15. Apparent fracture toughness v/s tempering temperature for quenched and tempered heat treatments.

Fig. 16. a) Scanning fractograph of as-quenched 52100 (treatment B-AQ) shows intergranular fracture with decohesion along prior austenite grain boundaries.

b) Scanning fractograph of as-quenched 52100+1Si (treatment B-AQ) shows failure by quasi-cleavage.

c) Fracture surface of as-quenched 52100+2Si (treatment B-AQ) shows quasi-cleavage facets.

Fig. 17. a) Scanning fractograph of quenched and tempered 52100 (B-T250) shows mixed mode of failure - intergranular + quasi-cleavage.

b) Fracture surface of quenched and tempered 52100+1Si (B-T250) shows failure by quasi-cleavage.

c) Fracture surface of quenched and tempered 52100+2Si (B-T250) shows failure by quasi-cleavage.

Fig. 18. Schematic of Schedule C - isothermal holding subsequent to low temperature austenitization.

Fig. 19. T.T.T. diagram of 52100 shows start (1%) and finish (99%) of transformation.

Fig. 20. T.T.T. diagram of 52100+1Si shows start (1%) and finish (99%) of transformation.

Fig. 21. T.T.T. diagram of 52100+2Si shows start (1%) and finish (99%) of transformation.

Fig. 22. a) Duplex microstructure of lower bainite and twinned martensite found in 52100 (treatment C-I255).

b) Fracture surface of 52100 (C-I255) shows mixed mode of fracture - partly intergranular and partly quasi-cleavage.

c) Lower bainitic microstructure of 52100 (treatment C-I305).

d) Fracture surface of 52100 (C-I305) shows failure by quasi-cleavage.

Fig. 23. a) Duplex microstructure observed in 52100+2Si (treatment C-I255) shows lower bainite and martensite.

b) Scanning fractograph of 52100+2Si (C-I255) shows quasi-cleavage facets.

c) Microstructure of 52100+2Si (C-I305) shows lower bainite.

d) Fracture surface of 52100+2Si (C-I305) shows mixed mode of failure - quasi-cleavage + dimpled rupture.

Fig. 24. Schematic of Schedule D - Two cycle austenitization treatments coupled with isothermal holding at different temperatures.

Fig. 25 a) Microstructure of 52100 (treatment D-I255) shows a mixture of lower bainites martensite and retained austenite.

b) Fracture surface of 52100 (D-I255) shows quasi-cleavage with no traces of intergranular fracture.

c) Microstructure of 52100 (D-I305).

d) Fracture surface of 52100 (D-I305) shows failure by quasi-cleavage.

Fig. 26. a) Microstructure of 52100+1Si (D-I255) shows lower bainite.

b) Quasi-cleavage observed in 52100+1Si (D-I255).

c) Microstructure of 52100+1Si (D-I305).

d) Fracture surface of 52100+1Si (D-I305) shows quasi cleavage.

Fig. 27. a) Microstructure of 52100+2Si (D-I255) contains lower bainite and martensite and retained austenite.

b) Fast fracture surface of 52100+2Si (D-I255) shows failure by quasi-cleavage.

c) Duplex microstructure of lower bainite + martensite with some retained austenite in 52100+2Si (D-I305).

d) Fracture surface of 52100+2Si (D-I305) shows quasi-cleavage.

Fig. 28. Hardness v/s percent Si addition for isothermal treatments C and D.

Fig. 29. Yield and ultimate tensile strengths v/s percent Si addition for isothermal treatments C and D. Data for some quenched and tempered treatments is also indicated for comparison.

Fig. 30. Calculated fracture toughness v/s percent Si addition for isothermal treatments C and D.

Fig. 31. Percent retained austenite v/s percent Si addition at different stages of tensile testing.

Fig. 32. Fracture toughness v/s yield strength for different heat treatments.

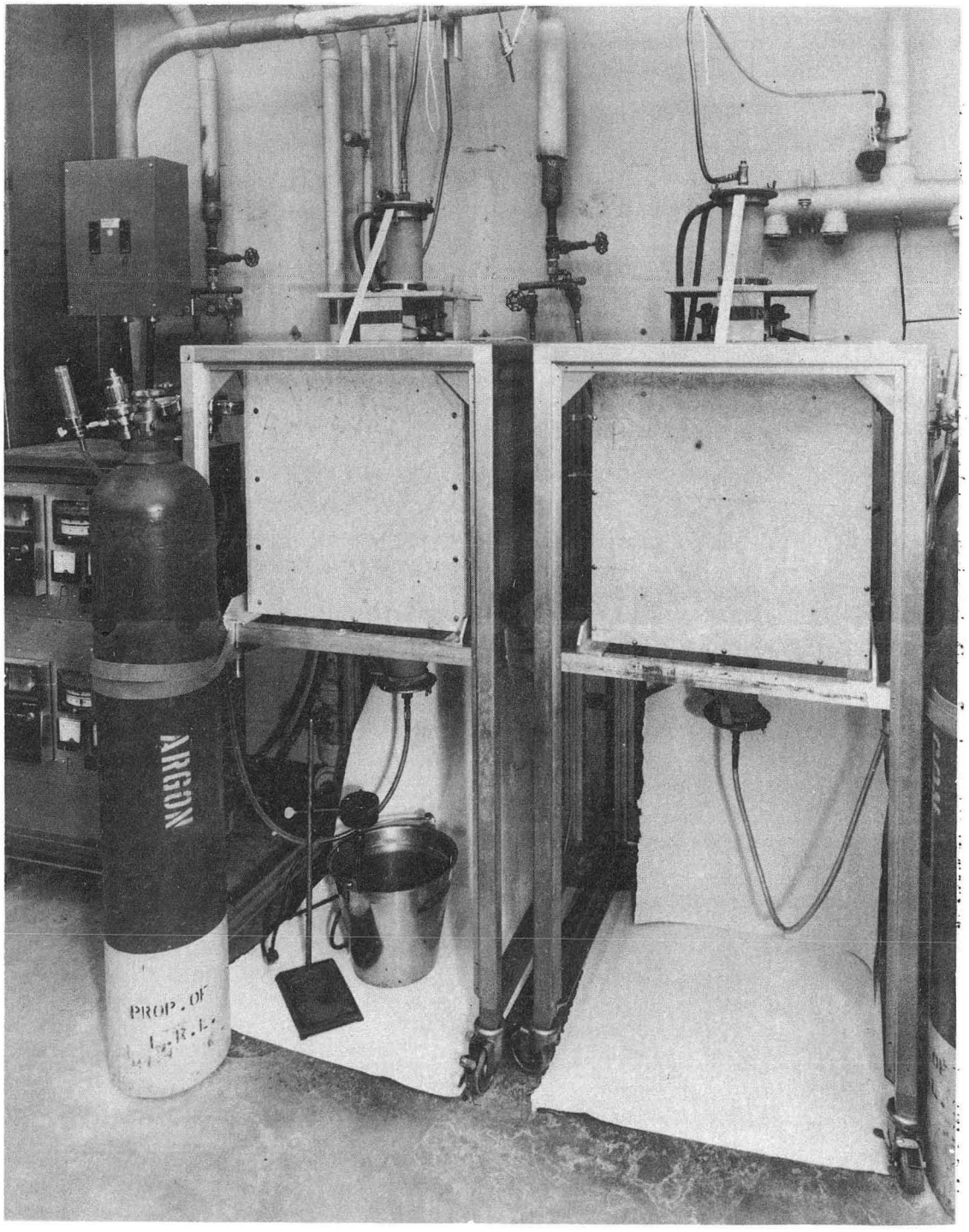

XBB 732-0504

Fig. 1.

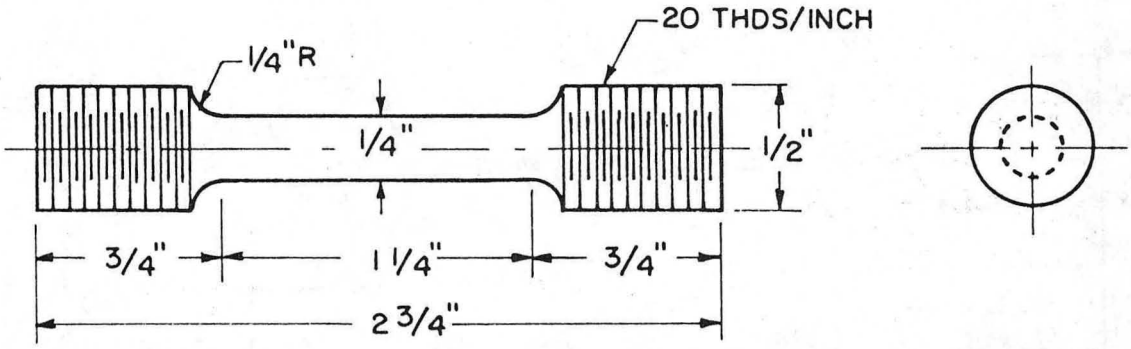

(b) ROUND TENSILE SPECIMEN

XBL 735-6189A

Fig. 2.

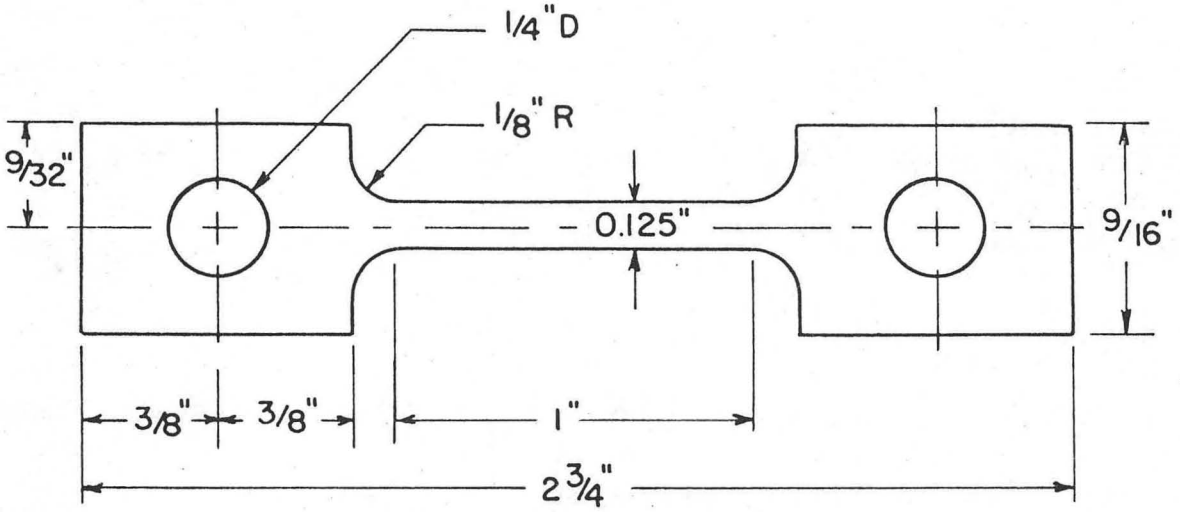

GAGE LENGTH: 1"
THICKNESS: 0.05"

TENSILE SPECIMEN

XBL 705-911

Fig. 3.

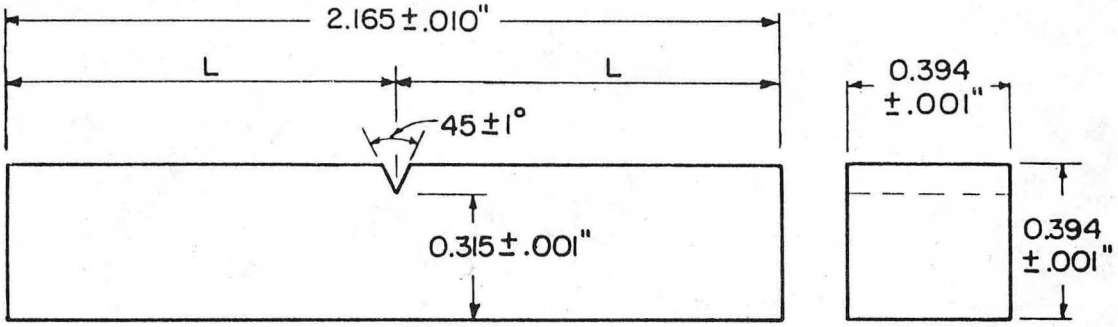

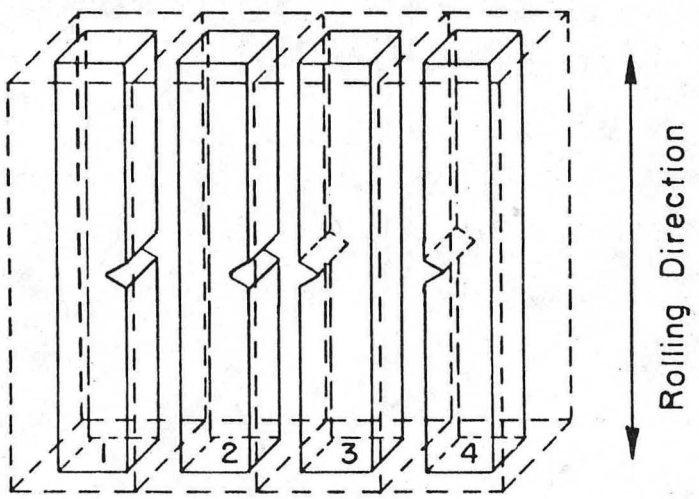

XBL 734-5988

Fig. 4.

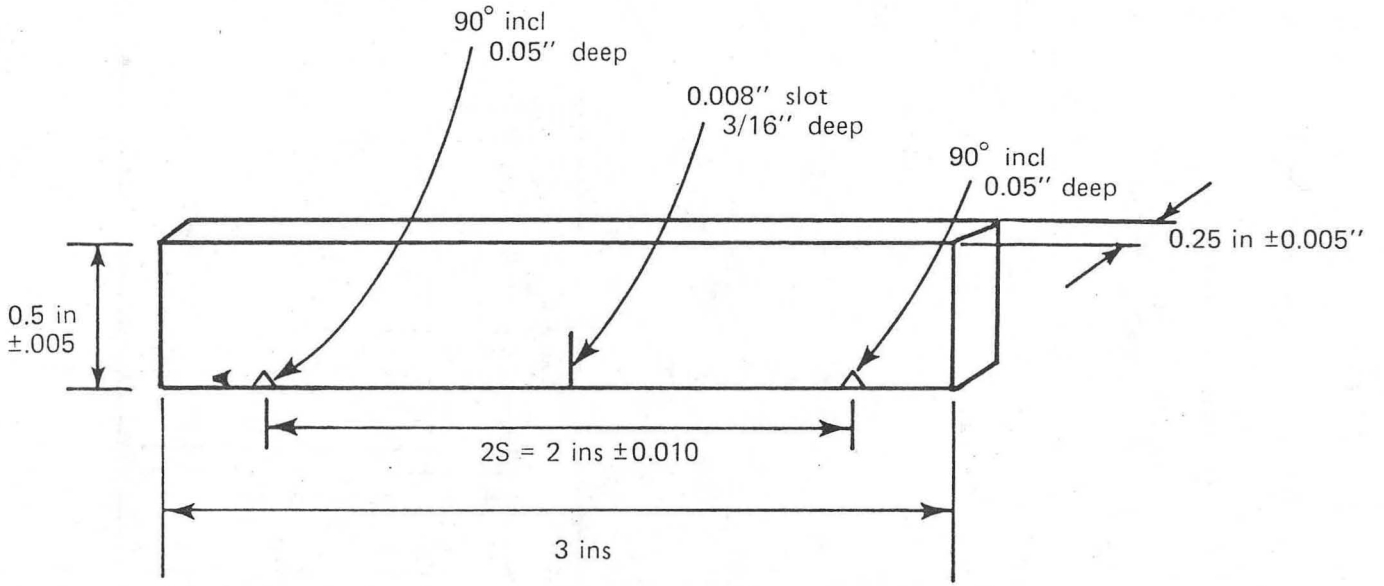

XBL 768-3300

Fig. 5.

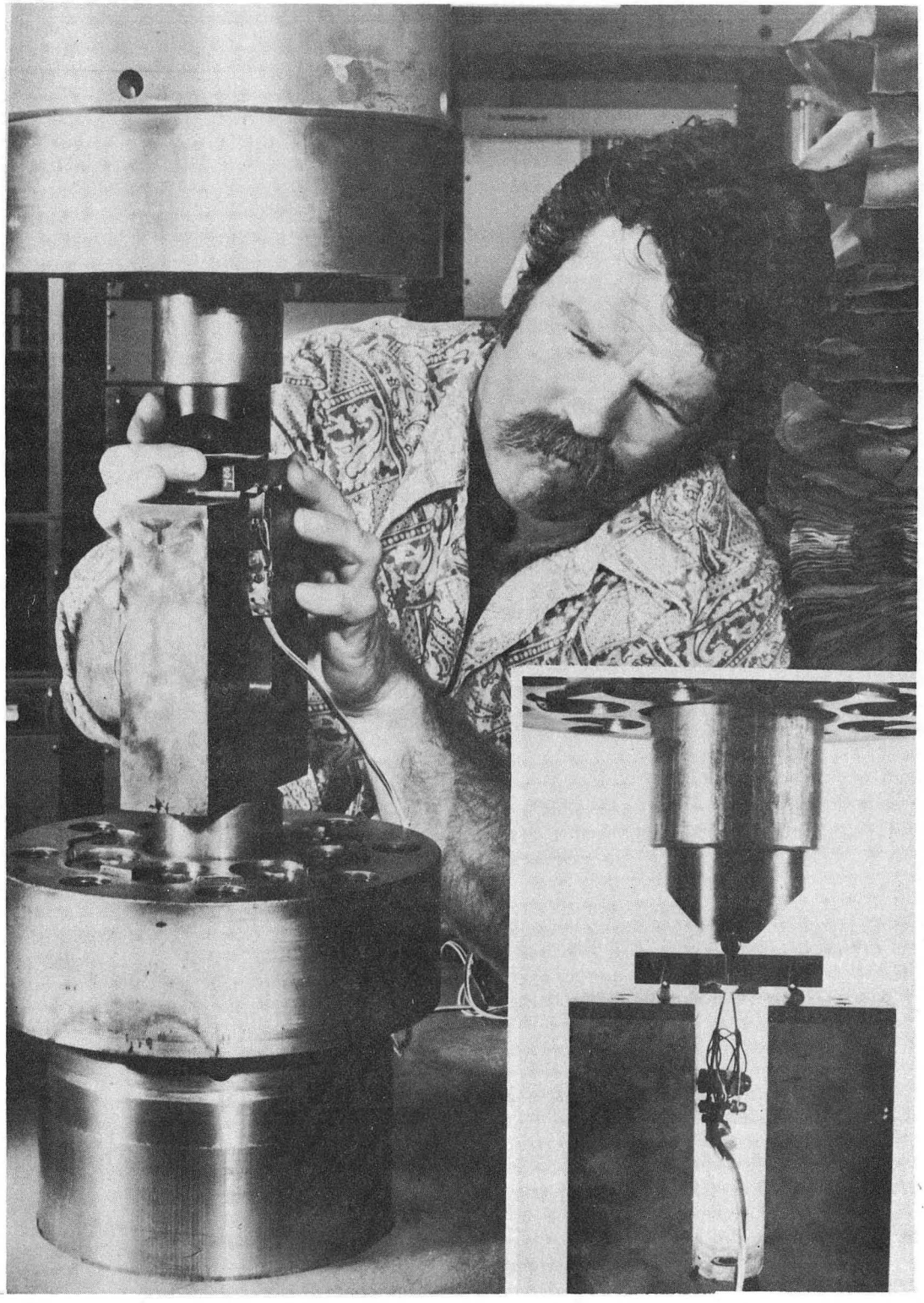

XBB 767-6740

Fig. 6.

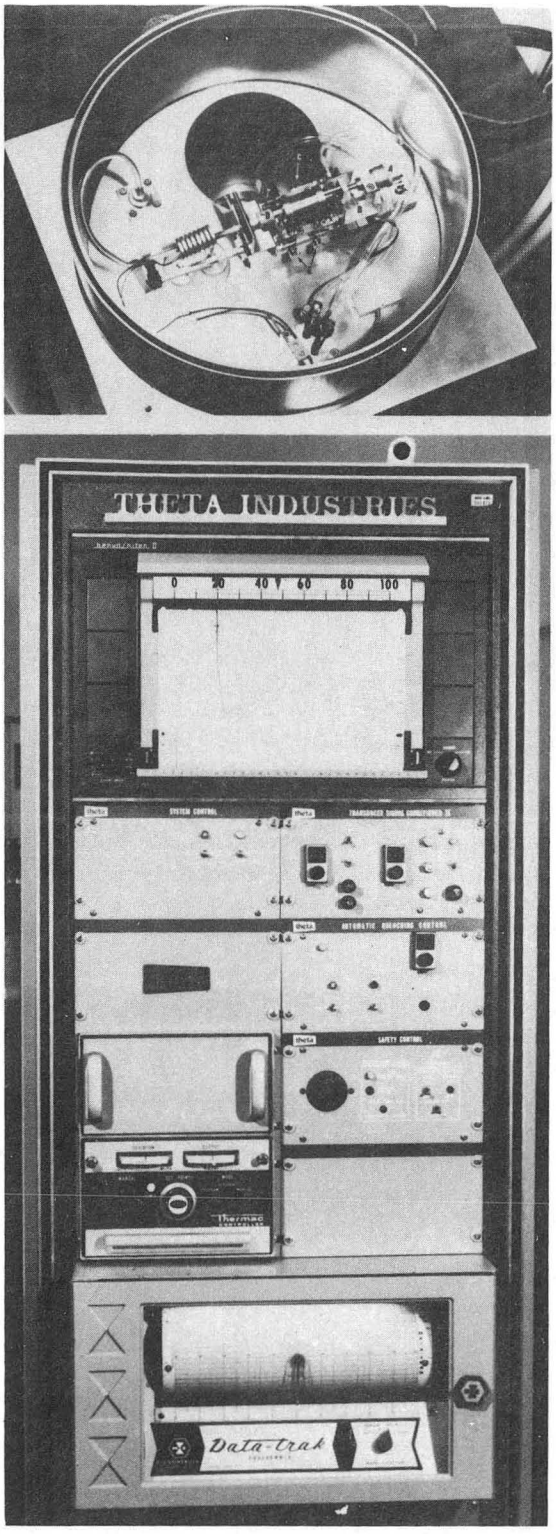

XBB 754-2369

Fig. 7.

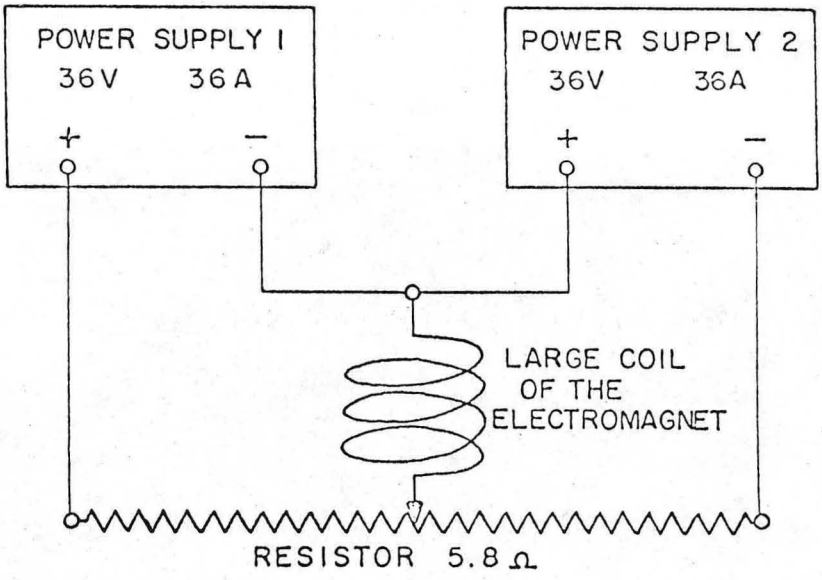

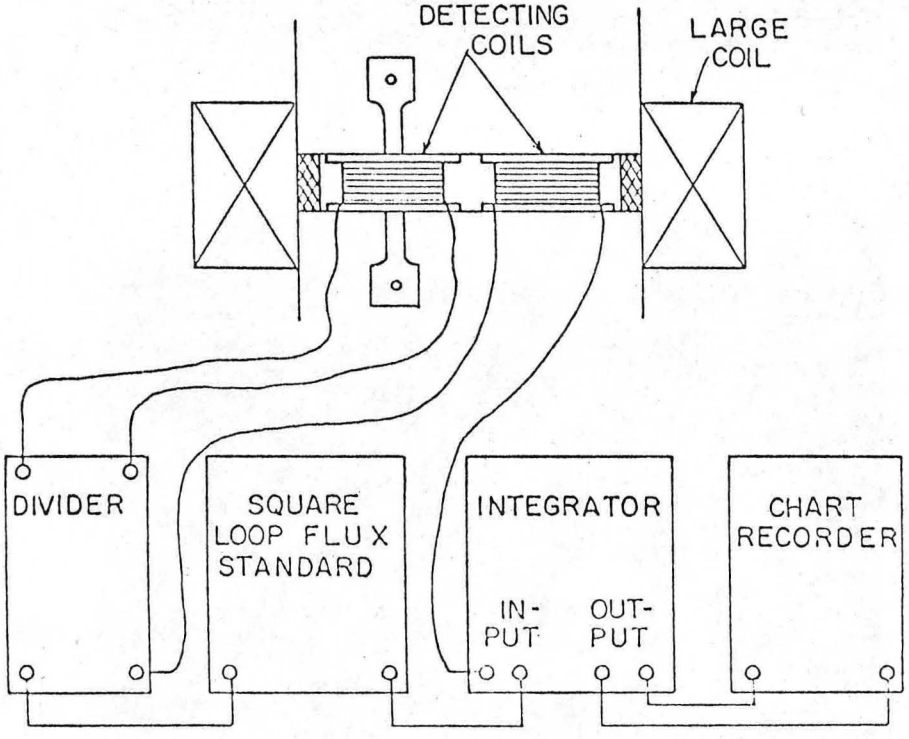

XBL 768-3308

Fig. 8.

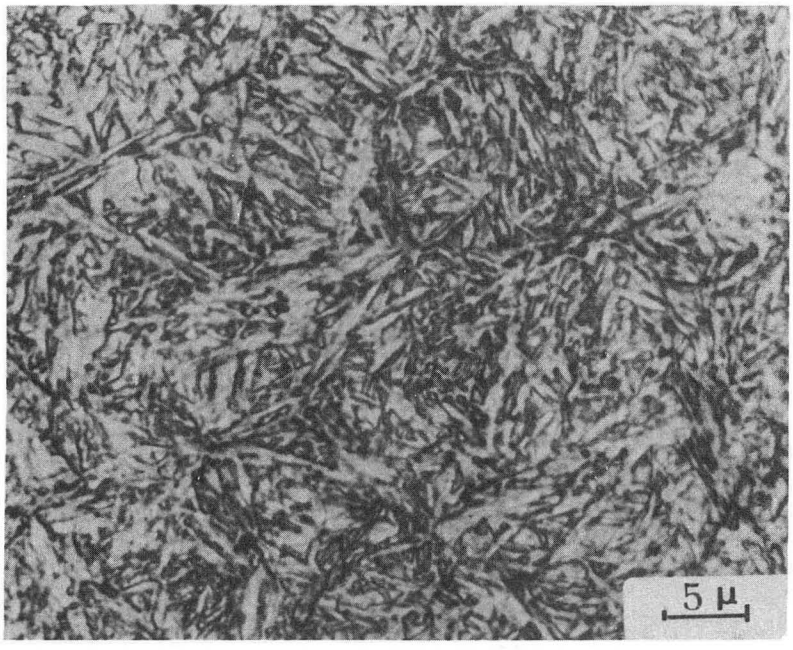

(a)

(b)

XBB 768-7549

Fig. 9.

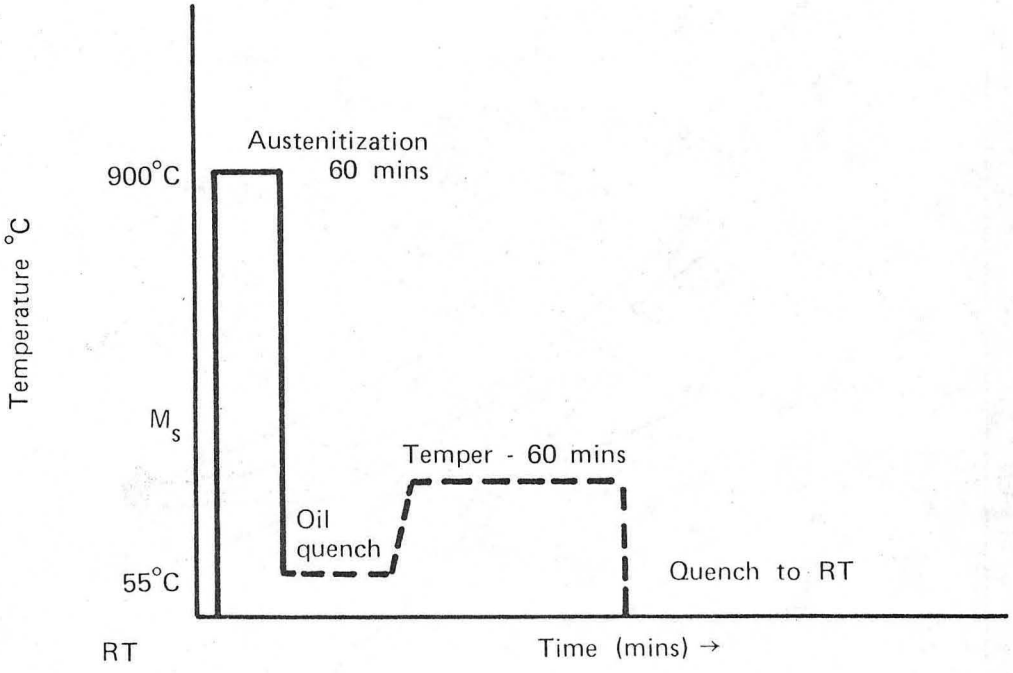

XBL 768-3296

Fig. 10.

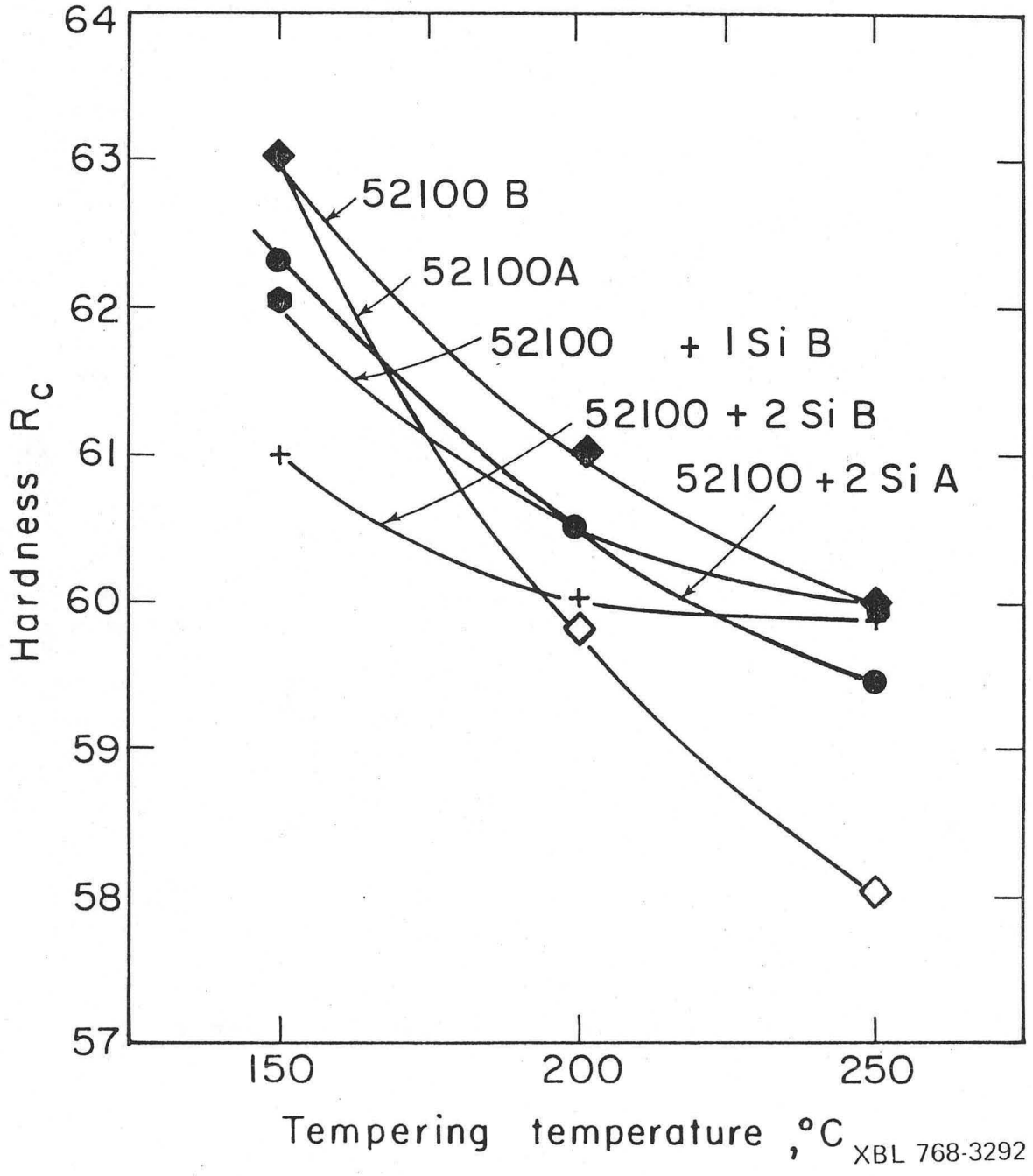
64
63
62
61
60
59
58
57
Hardness R_c
52100 B
52100A
52100 + 1Si B
52100 + 2 Si B
52100 + 2 Si A
150
200
250
Tempering temperature, °C
XBL 768-3292

Fig. 11.

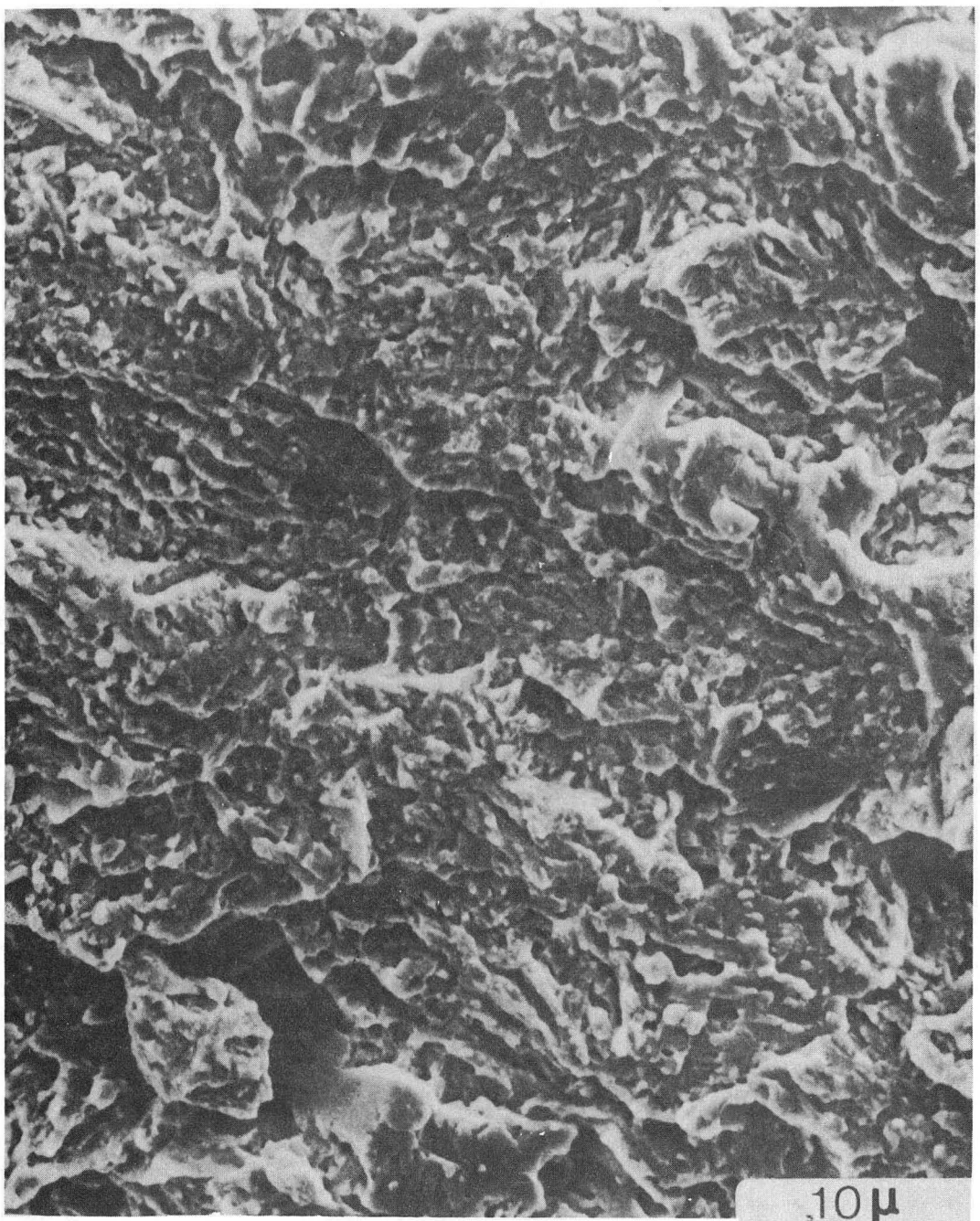

XBB 768-7550

Fig. 12.

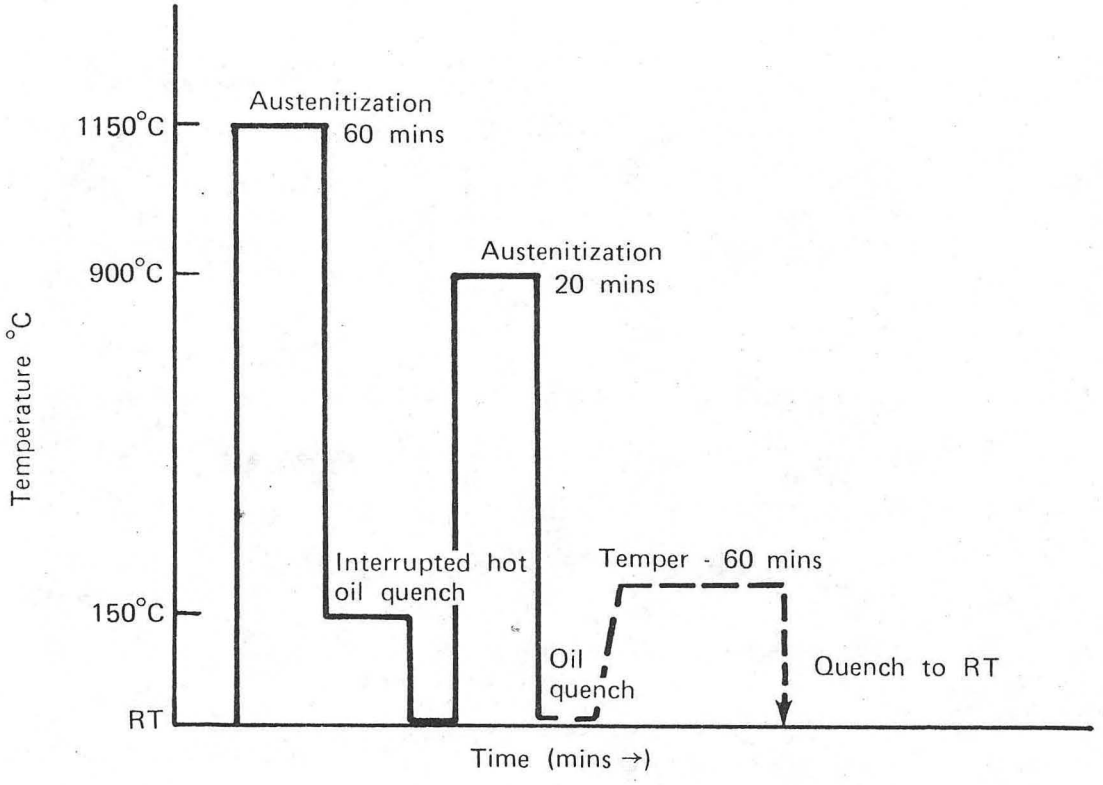

XBL 767-3298

Fig. 13.

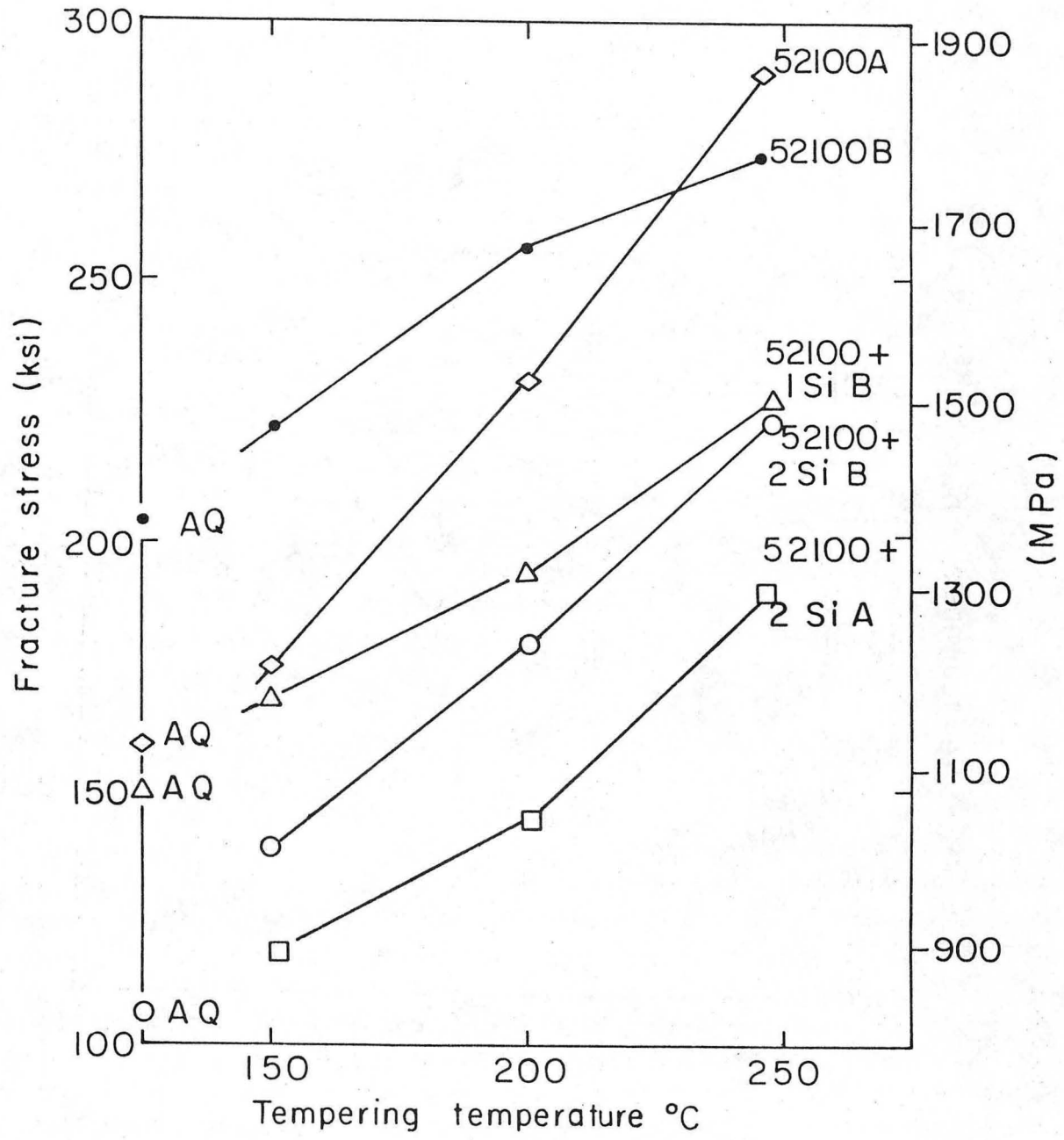

XBL 768-3306

Fig. 14.

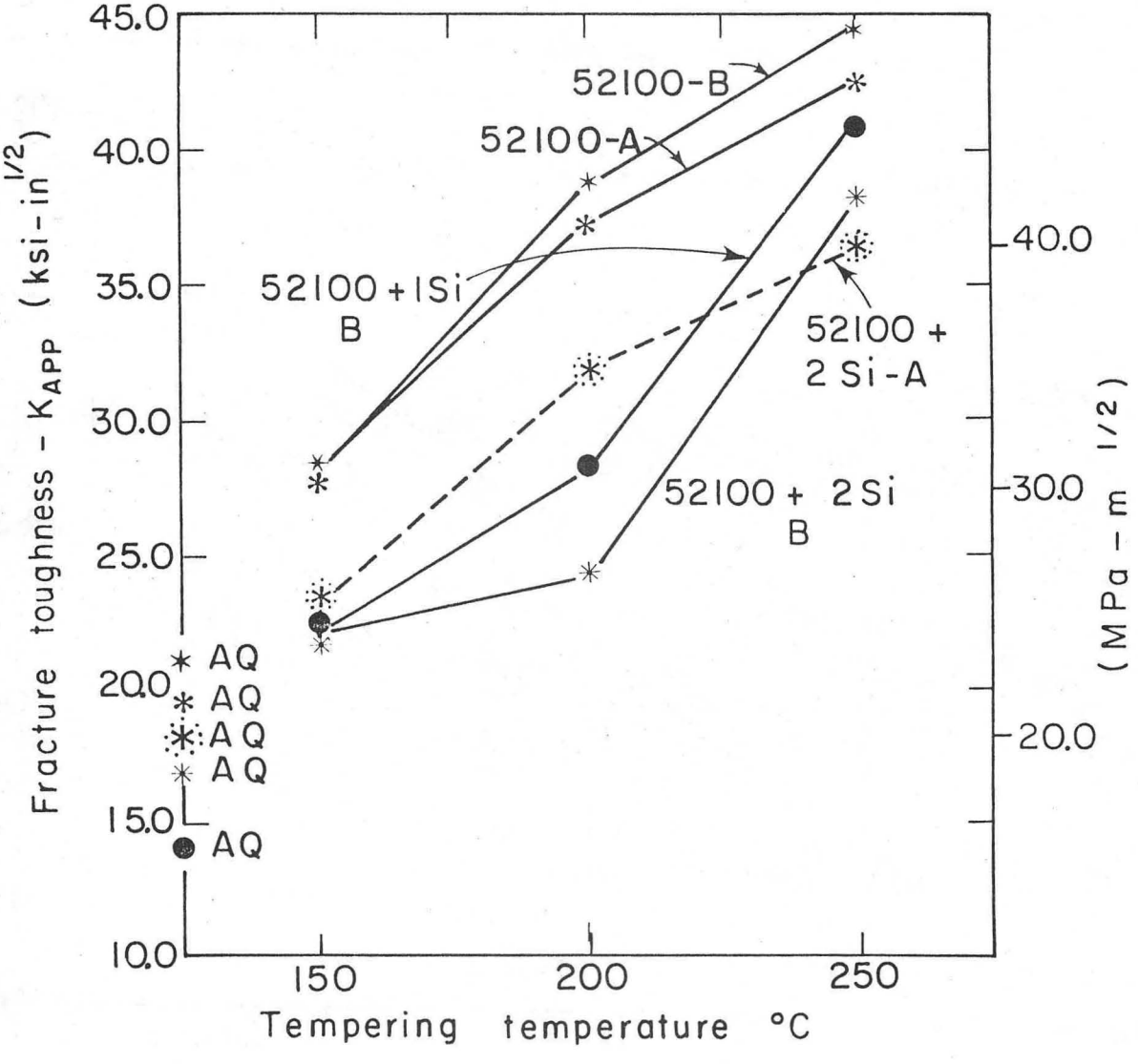
45.0
40.0
35.0
30.0
25.0
20.0
15.0
10.0
Fracture toughness - K_{APP} (ksi - $in^{1/2}$)
52100-B
52100-A
52100 + 1Si B
52100 + 2 Si-A
52100 + 2Si B
AQ
AQ
AQ
AQ
AQ
40.0
30.0
20.0
(MPa - $m^{1/2}$)
150
200
250
Tempering temperature °C
XBL 768 3287

Fig. 15.

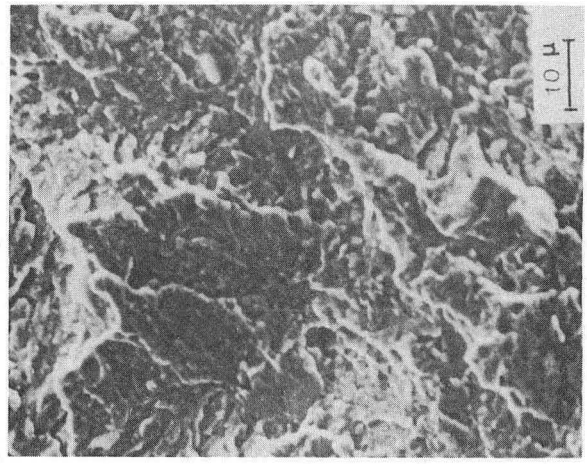

(c) XBB 768-7557

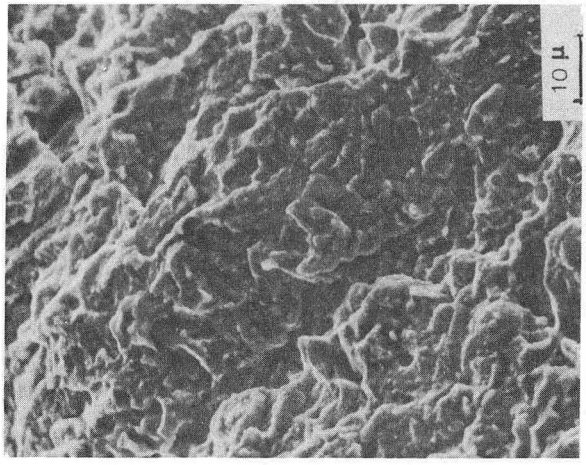

(b)

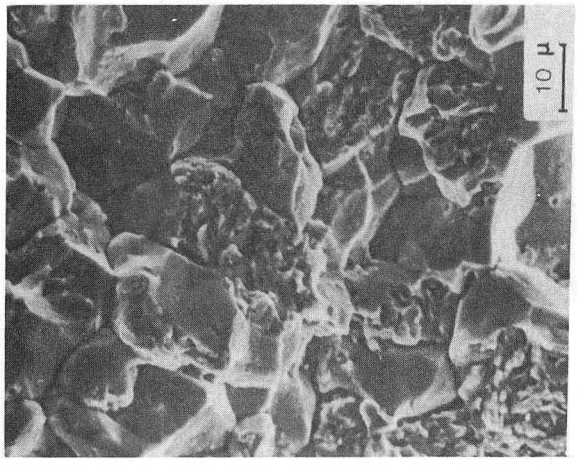

(a)

Fig. 16.

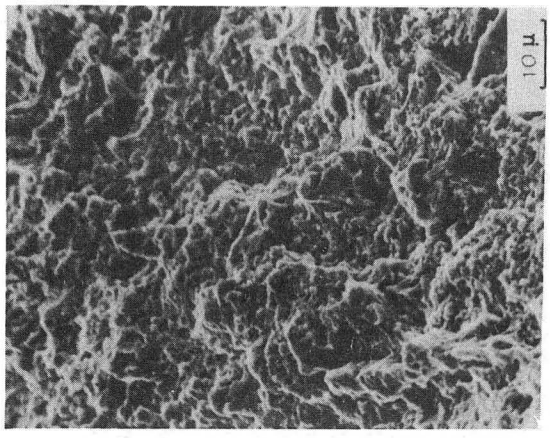

(c) XBB 768-7556

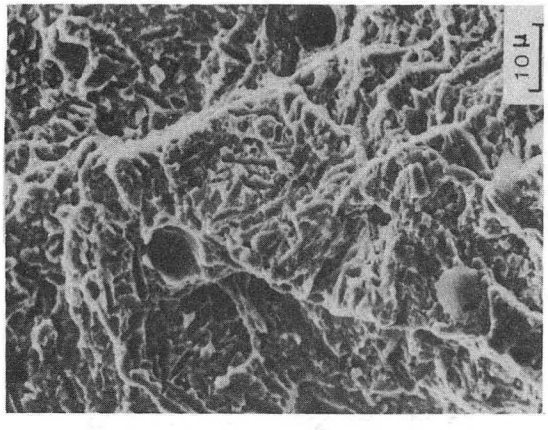

(b)

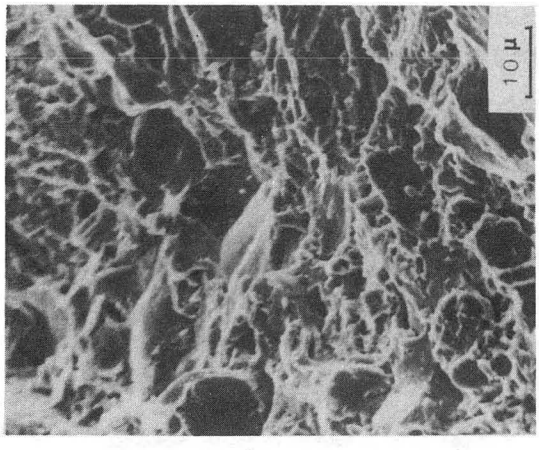

(a)

Fig. 17.

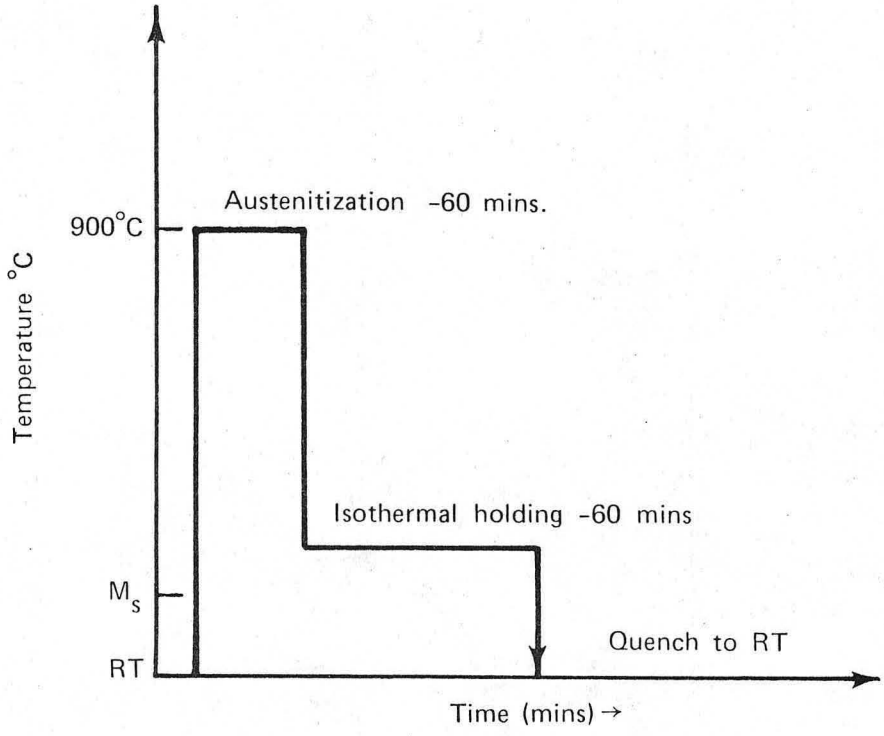

XBL 768-3297

Fig. 18.

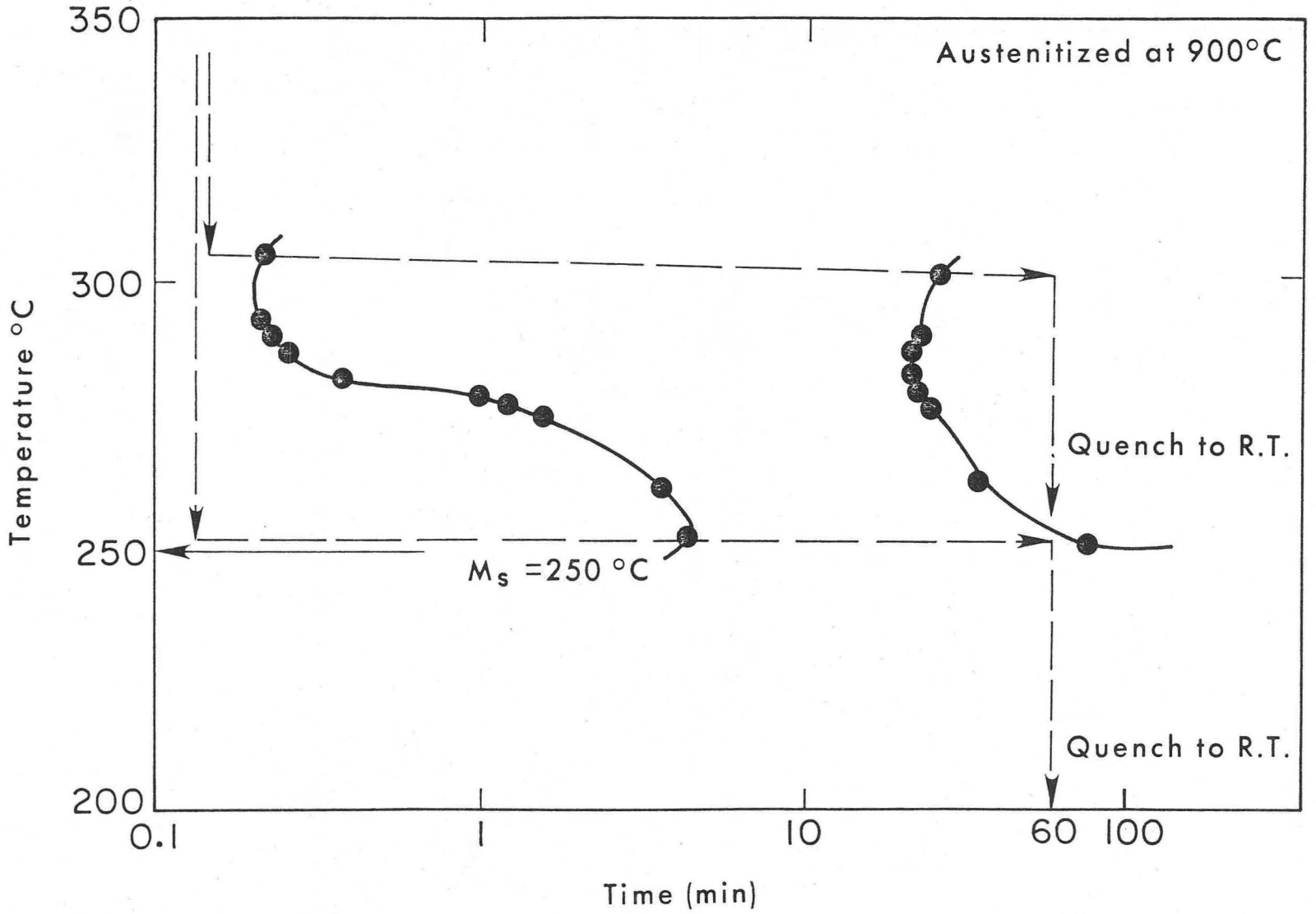

Fig. 19.

XBL 768-3289

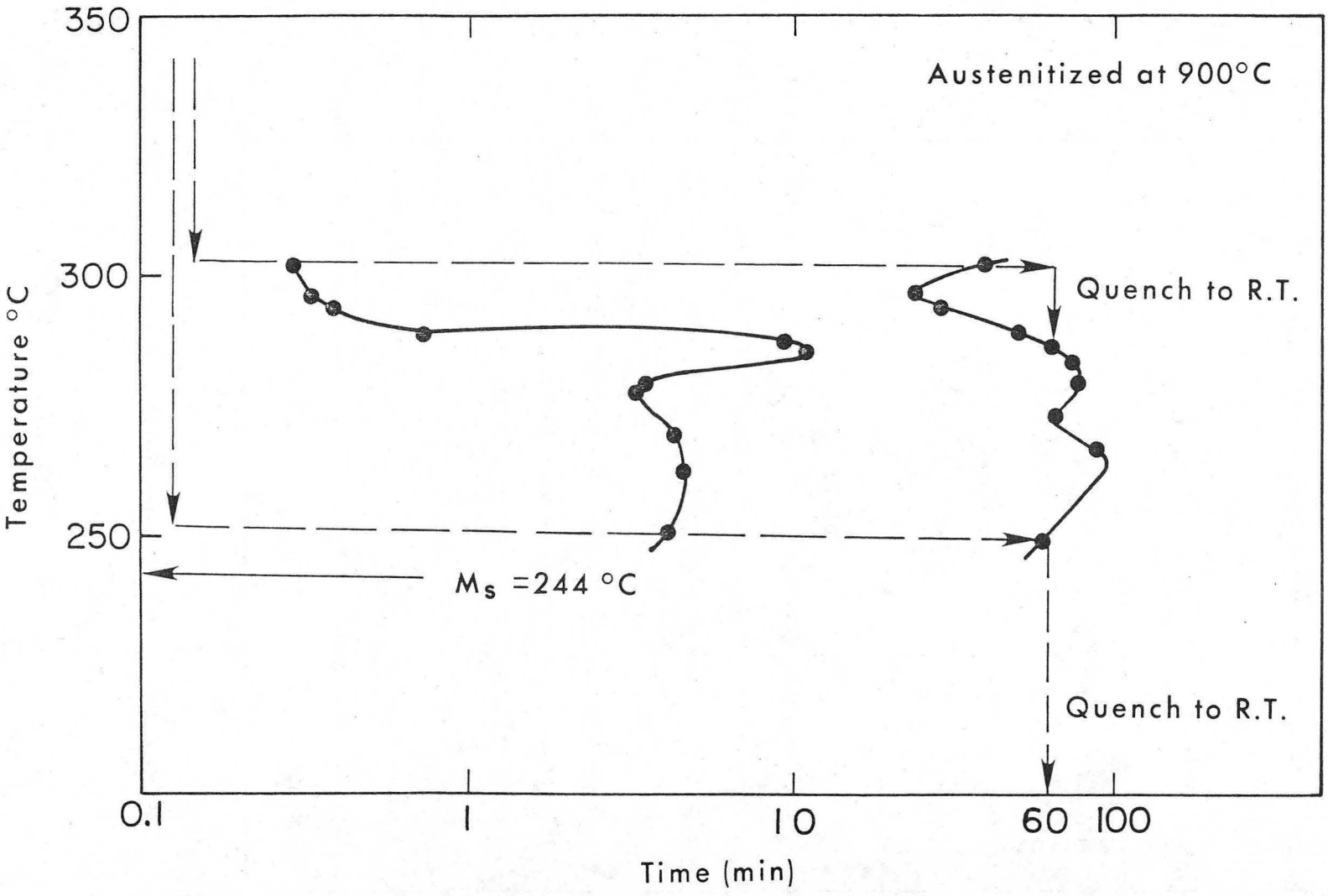

Fig. 20.

XBL 768-3288

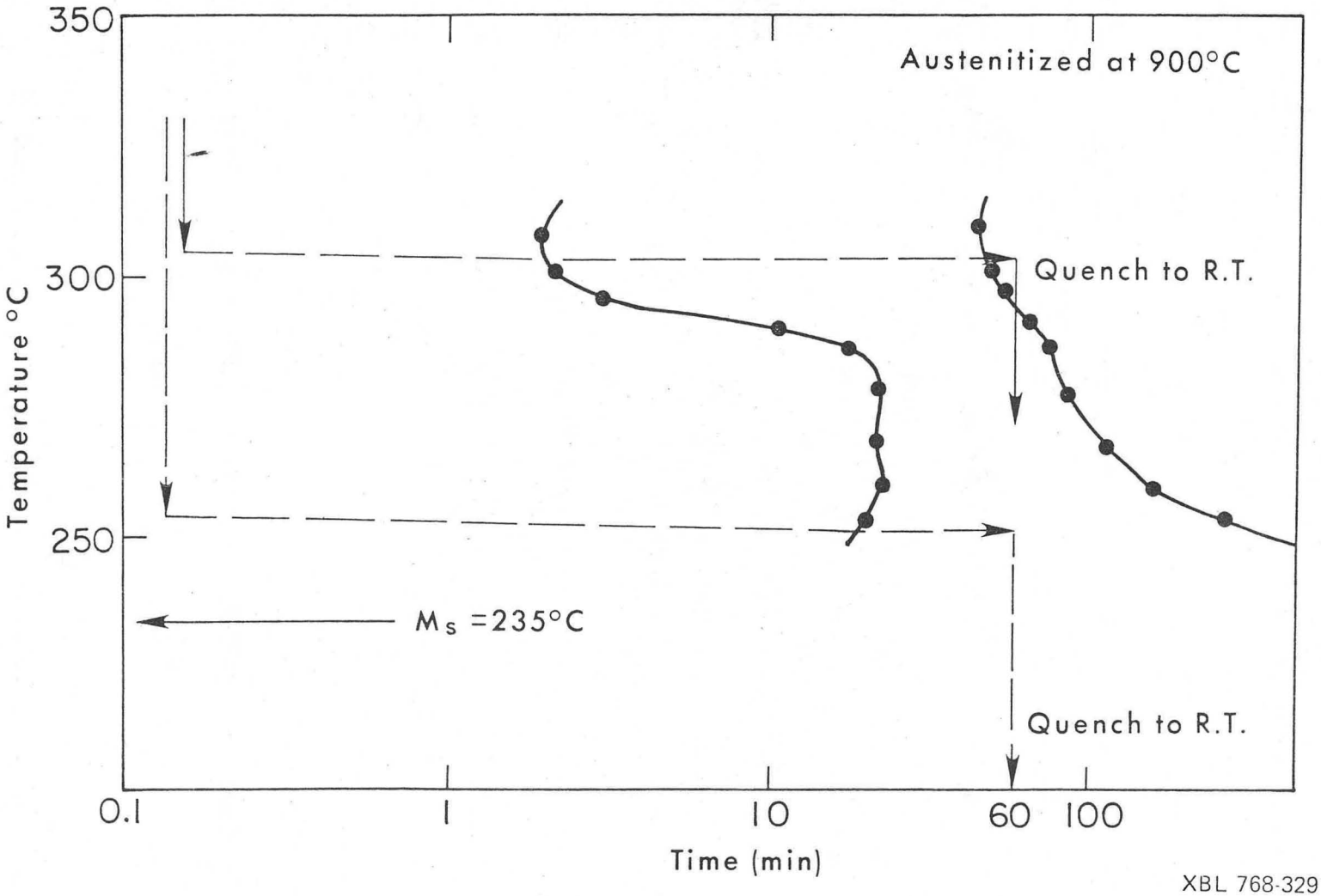
350
300
250
Temperature °C
Austenitized at 900°C
Quench to R.T.
M_s =235°C
Quench to R.T.
0.1
1
10
60
100
Time (min)
XBL 768-3291

Fig. 21.

(a)

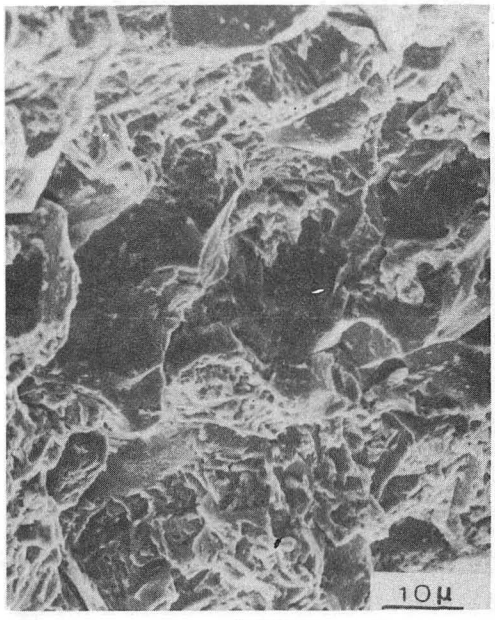

(b)

(c)

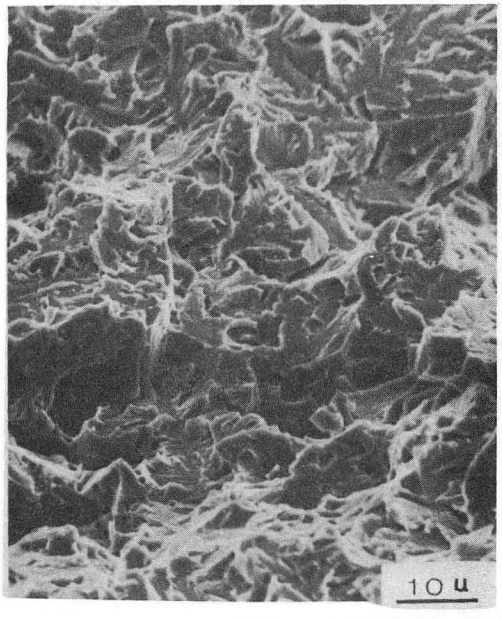

(d) XBB 768-7553

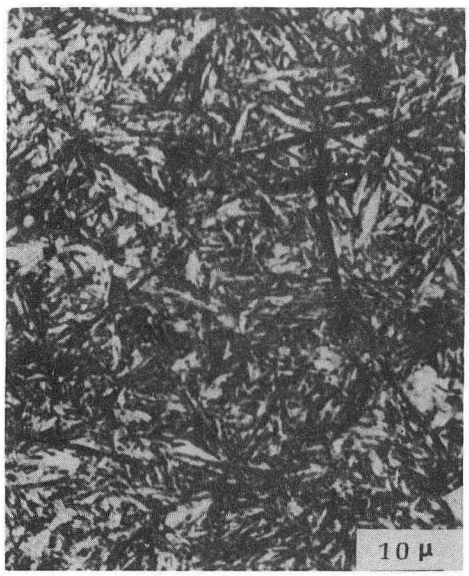

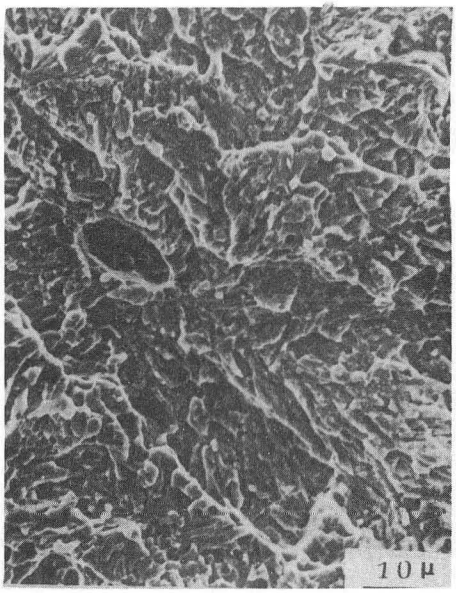

(b)

(c)

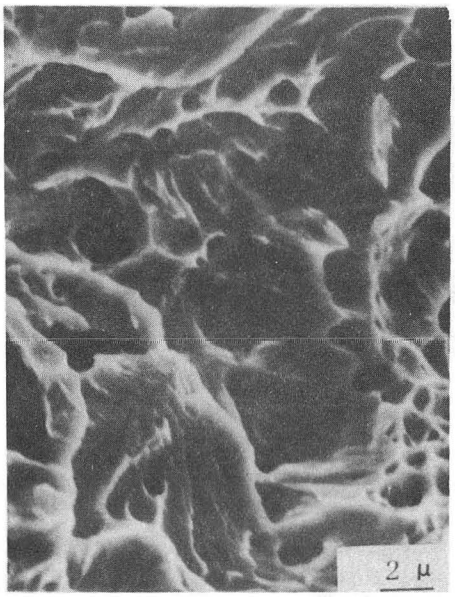

(d) XBB 768-7551

Fig. 23.

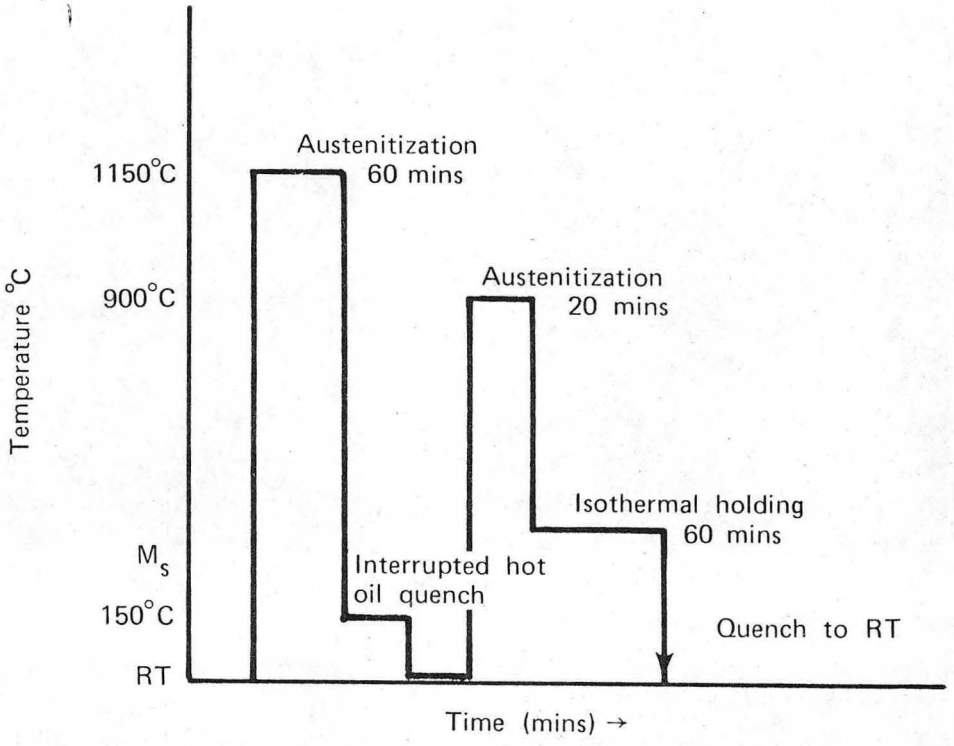

XBL 768-3299

Fig. 24.

(a)

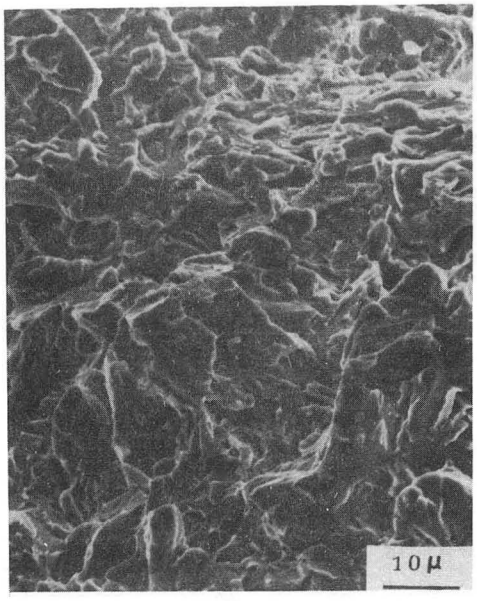

(b)

(c)

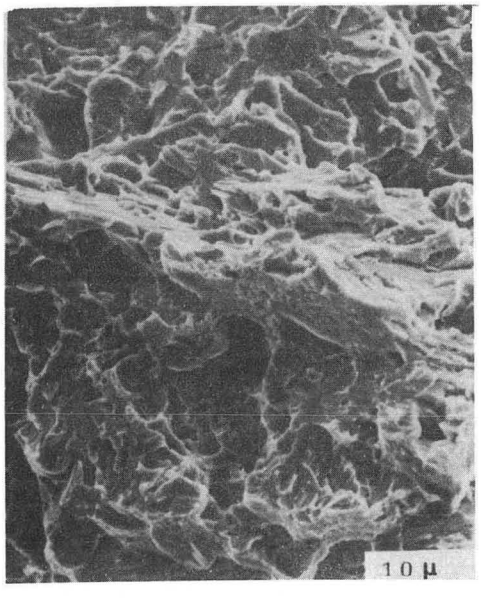

(d)

XBB 768-7552

Fig. 25.

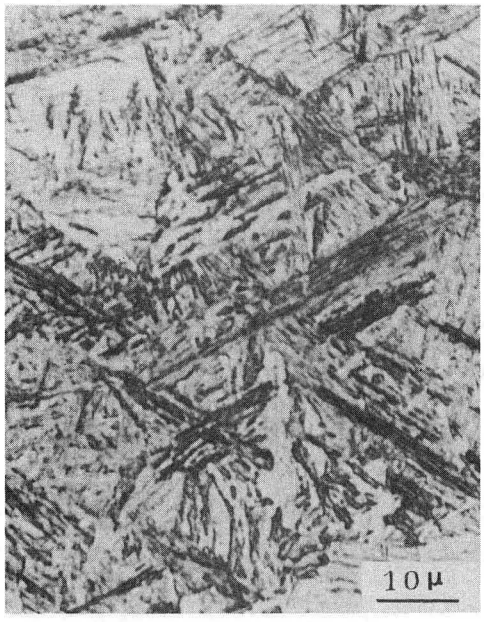

(a)

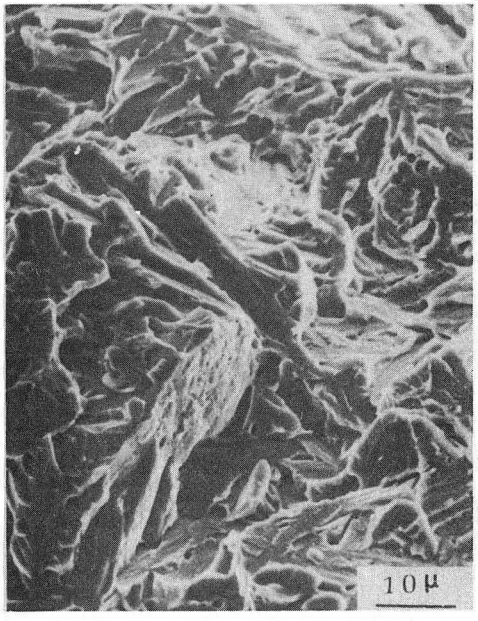

(b)

(c)

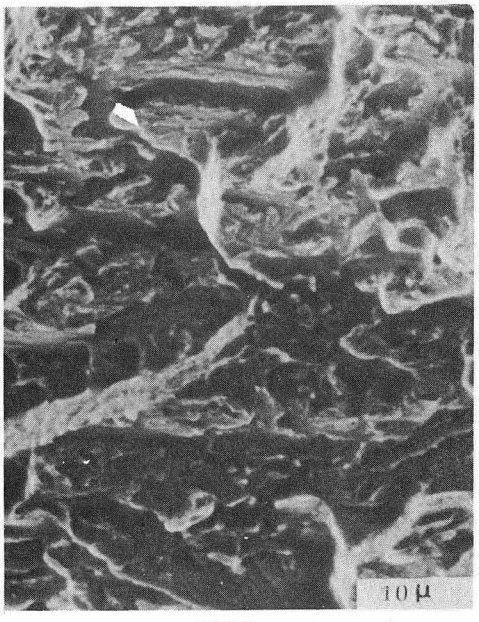

(d)

XBB 768-7554

Fig. 26.

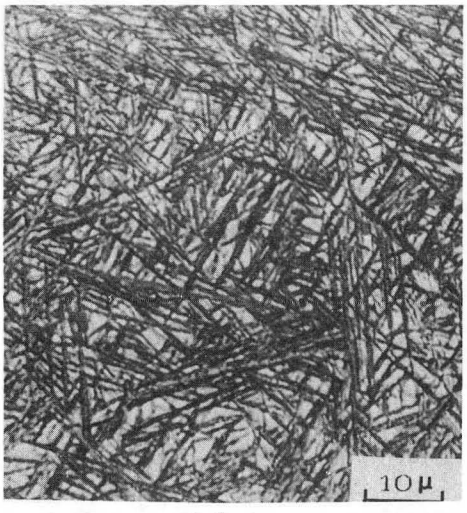

(a)

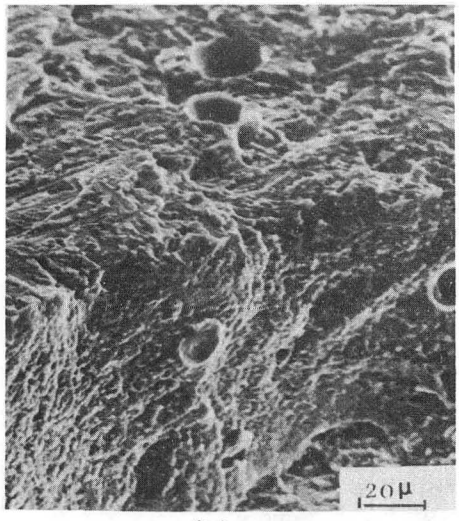

(b)

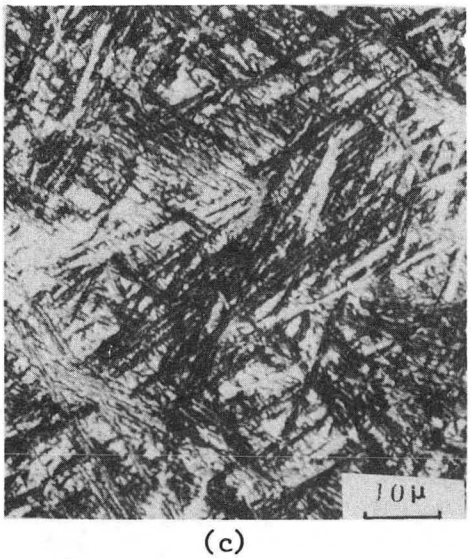

(c)

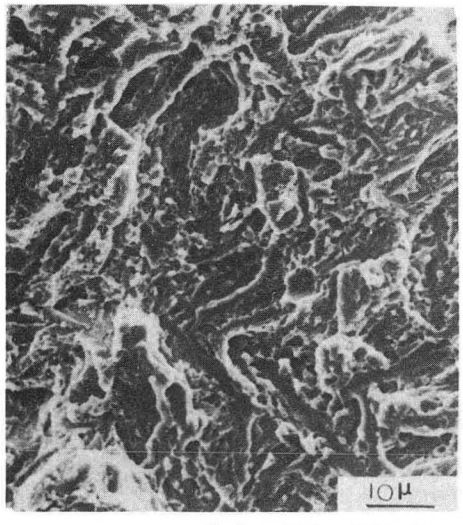

(c) XBB 768-7555

Fig. 27.

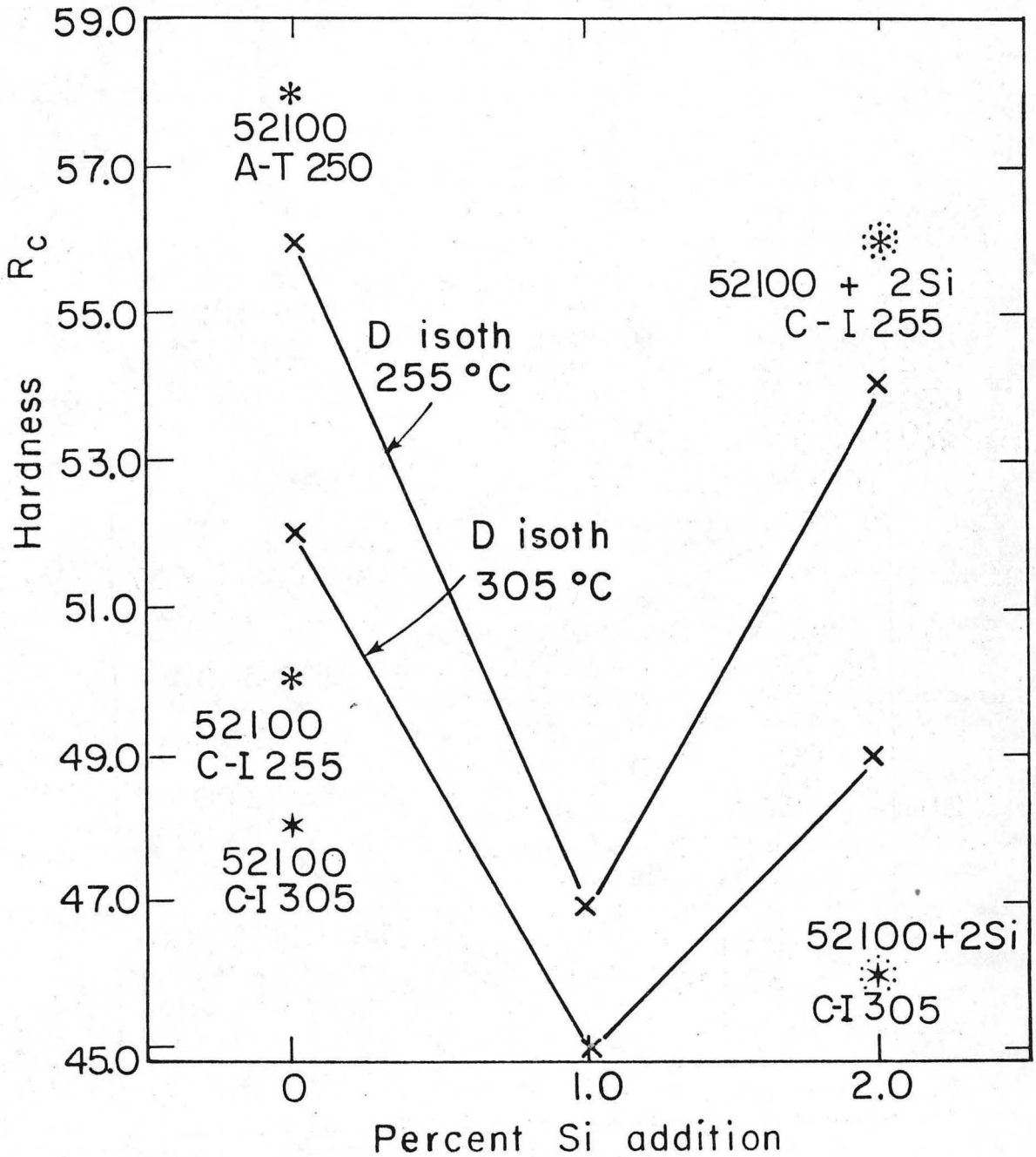

XBL 768-3293

Fig. 28.

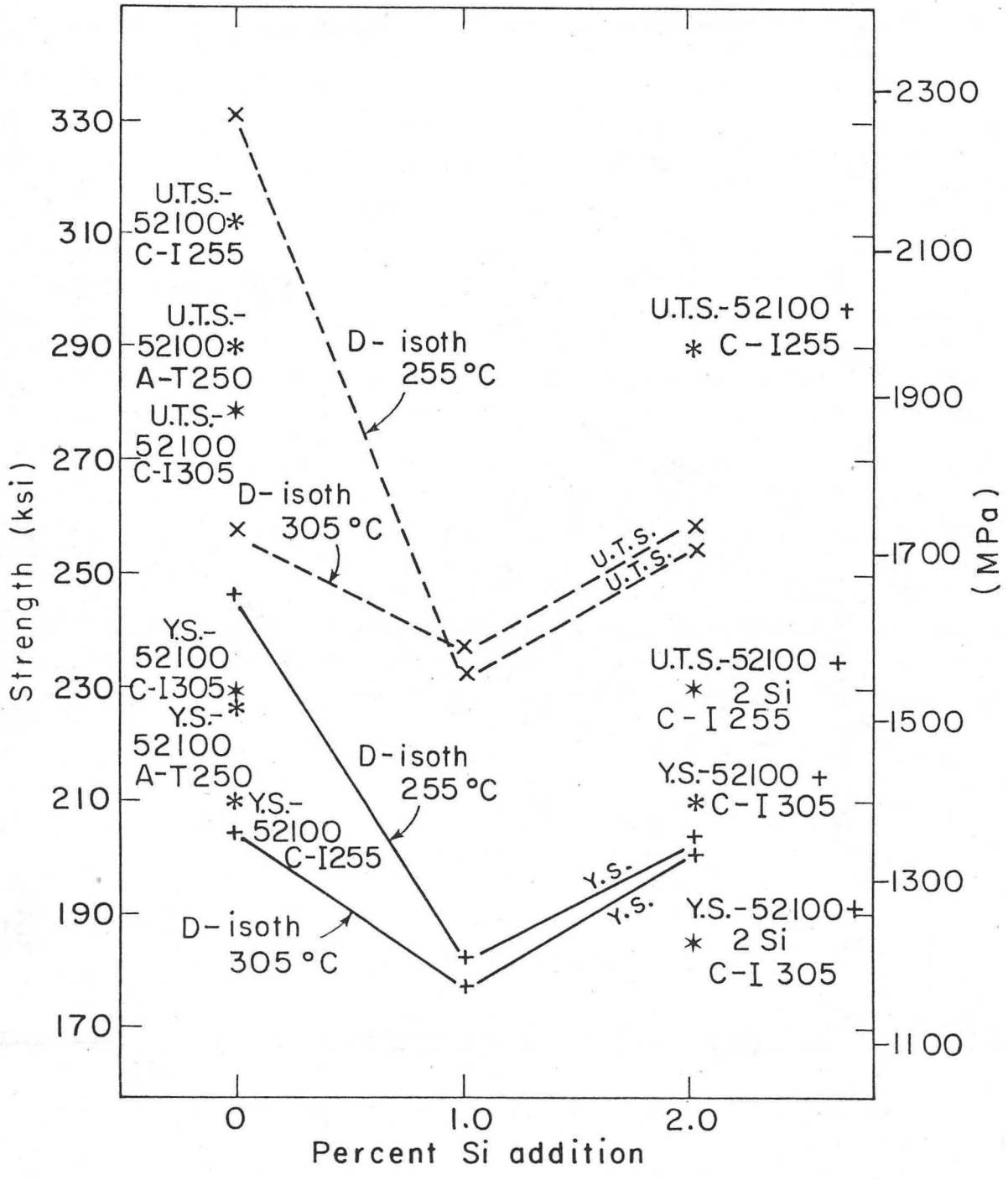

XBL 768-3314

Fig. 29.

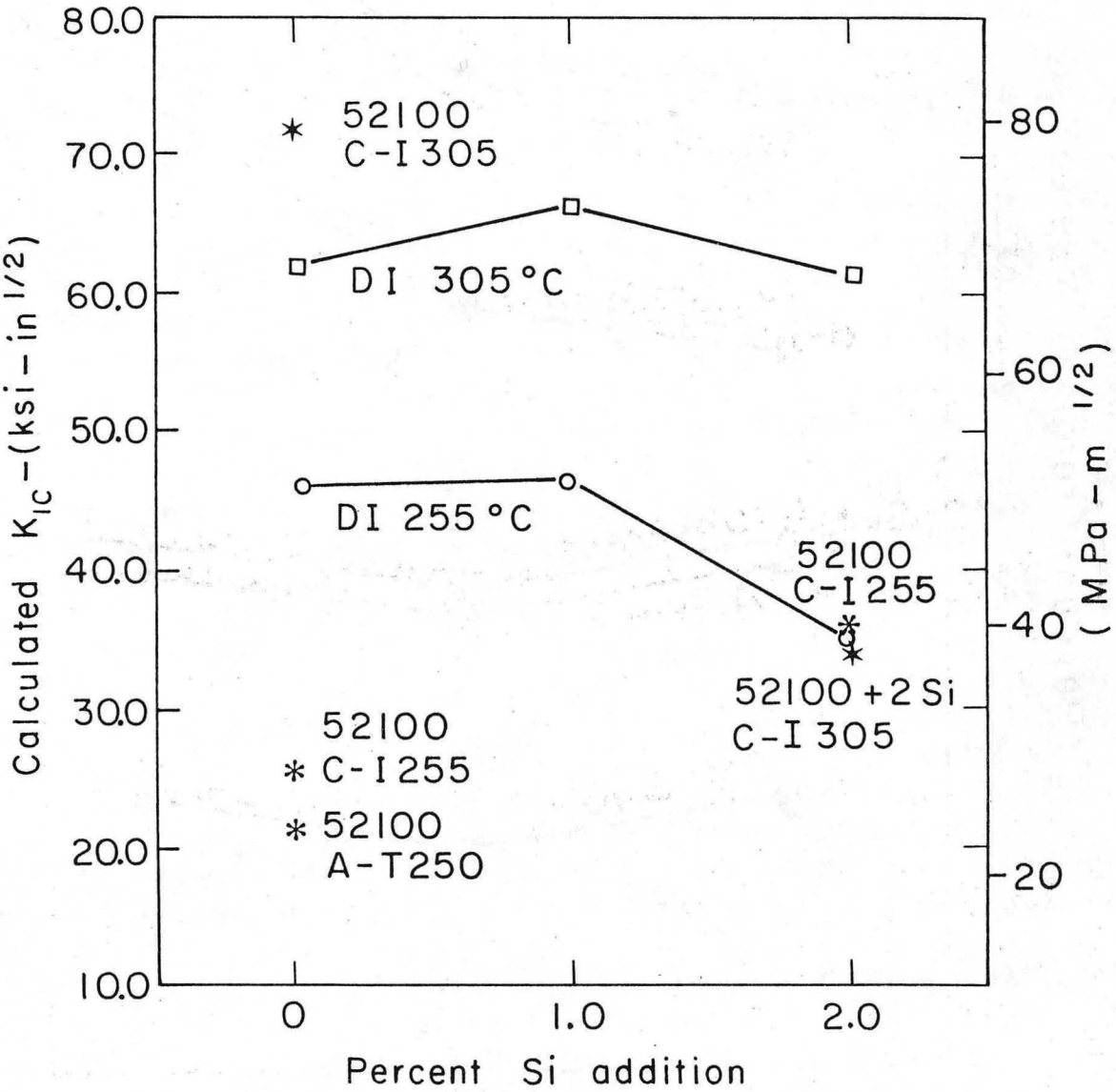

XBL 768-3301

Fig. 30.

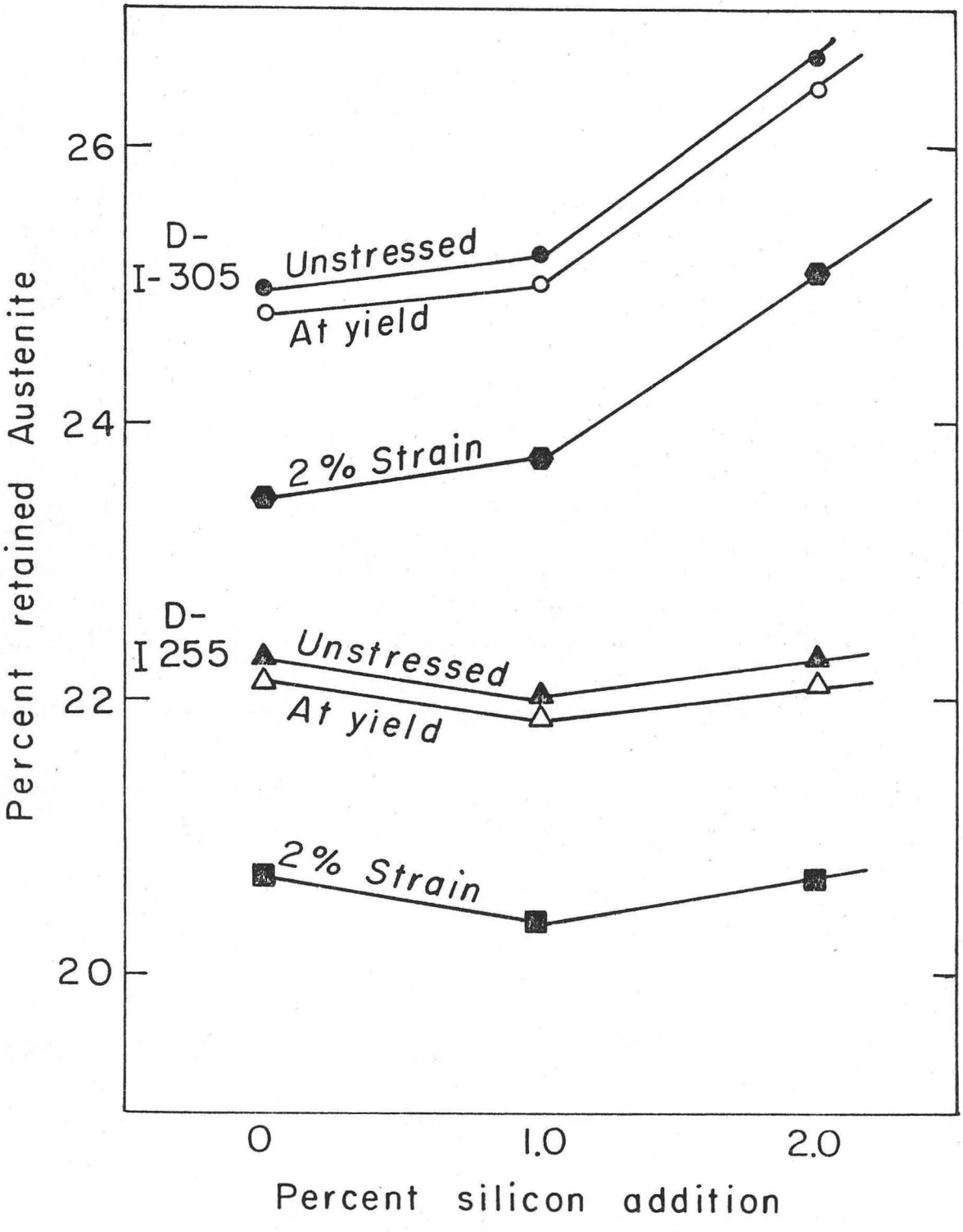

XBL 768-3321

Fig. 31.

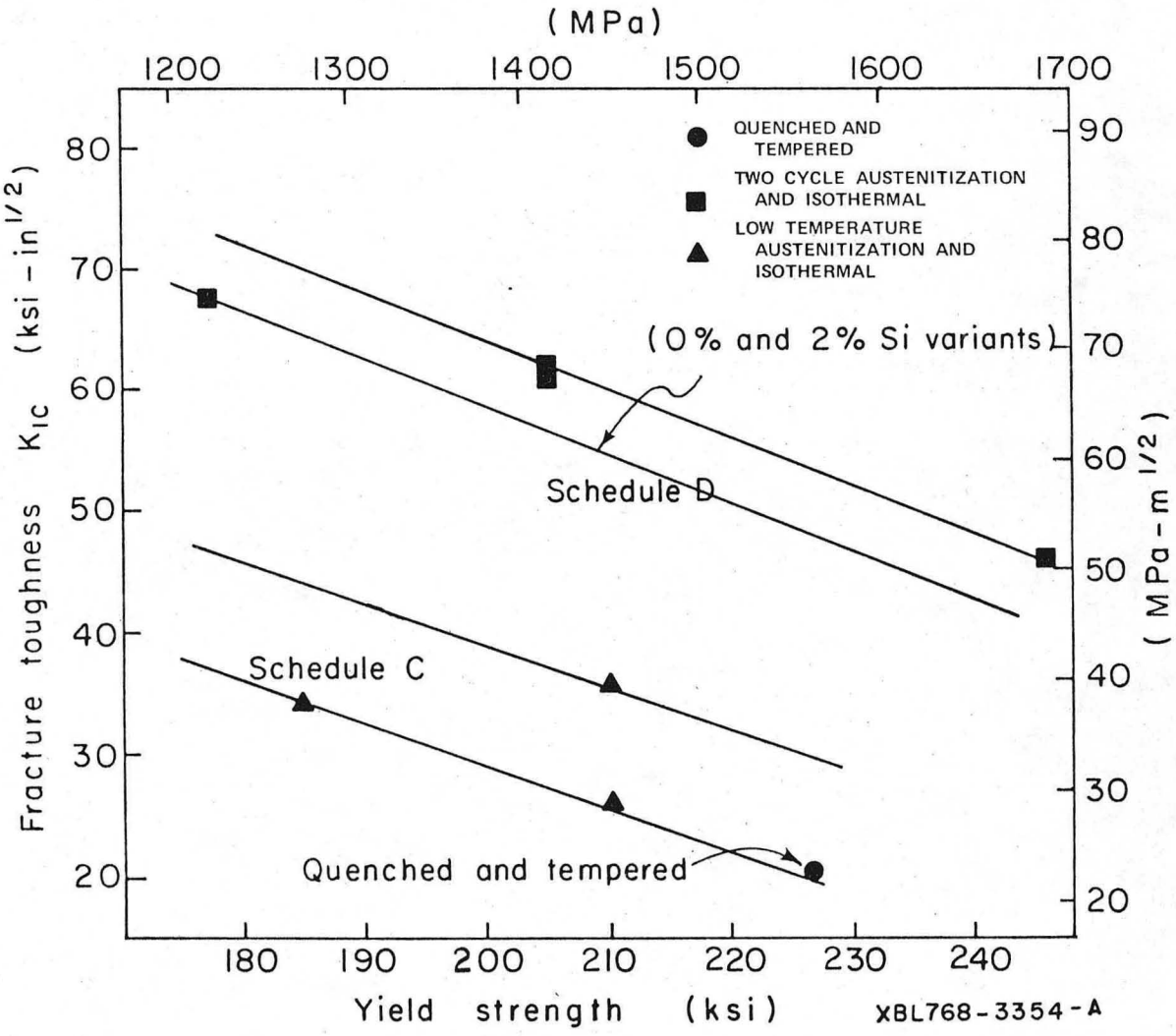

Fig. 32.

TECHNICAL INFORMATION DIVISION
LAWRENCE BERKELEY LABORATORY
UNIVERSITY OF CALIFORNIA
BERKELEY, CALIFORNIA 94720